Decadal Variability of Rainfall in Senegal: Beyond the Total Seasonal Amount

Aïssatou Badji, Elsa Mohino, Moussa Diakhaté, Juliette Mignot, Amadou Thierno Gaye

Decadal Variability of Rainfall in Senegal: Beyond the Total Seasonal Amount

AÏSSATOU BADJI,[a] ELSA MOHINO,[b] MOUSSA DIAKHATÉ,[a,c] JULIETTE MIGNOT,[d] AND AMADOU THIERNO GAYE[a]

[a] *Laboratoire de Physique de l'Atmosphère et de l'Océan-Siméon Fongang, École Supérieure Polytechnique, Université Cheikh Anta Diop, Dakar, Sénégal*
[b] *Departamento de Física de la Tierra y Astrofísica, Facultad de Ciencias Físicas, Universidad Complutense de Madrid, Madrid, Spain*
[c] *École Supérieure des Sciences et Techniques de l'Ingénieur, Université Amadou Mahtar Mbow de Diamniadio, Diamniadio, Sénégal*
[d] *Laboratoire d'Océanographie et du Climat: Expérimentations et Approches Numériques, Institut Pierre Simon Laplace, SU/IRD/CNRS/MNHN, UMR 7159, Paris, France*

(Manuscript received 6 September 2021, in final form 30 March 2022)

ABSTRACT: Rainfall characteristics are crucial in monsoon regions, in particular for agriculture. Crop yields indeed depend on the rainfall seasonal amounts, but also on other rainfall characteristics such as the onset of the rainy season or the distribution of rainy days. In the Sahel region, while the average amount of seasonal rainfall has been shown to be marked by strong decadal variability, the modulation of rainfall characteristics has received less attention in the literature so far. In this study, we show that the frequency of light, heavy, and extreme rainfall events and the mean intensity of rainfall events in Senegal exhibit a marked decadal variability over the 1918–2000 period, strongly similar to that of the mean seasonal rainfall. The decadal modulations of these events show a strong and positive link with the Atlantic multidecadal variability (AMV). Indeed, positive sea surface temperature anomalies over the North Atlantic and Mediterranean related to a warm AMV phase are associated with negative sea level pressure anomalies over the northern Atlantic and a northward shift of the intertropical convergence zone. We also find that the onset and cessation dates as well as the length of the rainy season show relatively less decadal variability, which is more related to the interdecadal Pacific oscillation (IPO), a positive phase of the latter leading to a late onset, an early cessation, and an overall shorter rainy season in Senegal.

KEYWORDS: Africa; Extreme events; Monsoons; Precipitation; Decadal variability

1. Introduction

The Sahel is a semi-arid region of North Africa located between latitudes 10° and 20°N. The rainfall in this region experiences significant variability at different time scales. Many authors have described and studied the variability of Sahelian rainfall at intraseasonal (e.g. Sultan et al. 2003; Maloney et Shaman 2008; Gaetani et al. 2010; Janicot et al. 2011), interannual (e.g. Losada et al. 2010; Rodríguez-Fonseca et al. 2011; Mohino et al. 2011b; Rodríguez-Fonseca et al. 2015), and decadal time scales (e.g. Folland et al. 1986; Palmer 1986; Giannini et al. 2003; Mohino et al. 2011a) as well as future projections of Sahel rainfall trends (e.g. Biasutti 2013).

The decadal variability of the seasonal amount of rainfall in the Sahel is very high, representing approximately 50% of the total year-to-year rainfall variance (Kitoh et al. 2020). Several studies have highlighted the fundamental role of sea surface temperatures (SSTs) for this decadal variability (Folland et al. 1986; Palmer 1986; Rowell et al. 1992; Giannini et al. 2003; Lu and Delworth 2005; Mohino et al. 2011a). Mohino et al. (2011a) have related the decadal variability of rainfall in the Sahel during the twentieth century to the joint influence of the Atlantic multidecadal variability (AMV), the interdecadal Pacific oscillation (IPO), and the long-term global warming (GW) SST trend. In addition, recent studies have suggested that anthropogenic aerosols are the primary driver of the forced Sahelian rainfall decadal variability in the late twentieth century (Hirasawa et al. 2020; Marvel et al. 2020; Bonfils et al. 2020). However, the decadal variability of rainfall characteristics in the Sahel over the historical period has received less attention in the literature so far. This could be explained in part by the unavailability of sufficiently long time series of daily rainfall data. Nevertheless, rainfall characteristics have important implications on Sahelian agriculture and are relevant for effective planning. For example, the development and yield of millet, sorghum, and maize depend on the rainfall amount, the onset and cessation dates of the rainy season, and the seasonal distribution of rainy days and dry spells (Misra and Misra 1991; Le Houerou 1992; Sivakumar 1992; Oladipo and Kyari 1993; Sultan et al. 2005). Moreover, some rainfall characteristics such as extreme storms have shown strong changes in recent decades (Taylor et al. 2017).

Among the few existing studies, Salack et al. (2014) showed that at interannual time scales, dry spell occurrence over the Sahel is linked to anomalously warm SSTs over the Atlantic, Pacific, and Indian Oceans. When the global tropics and the tropical Atlantic are warmer than normal, one can note more dry spells. In contrast, dry spells decrease when concurrently the equatorial South Atlantic is warmer than normal and, especially, the Indo-Pacific is cooler. Diakhate et al. (2019) have shown that the occurrence of Sahel moderate daily rainfall (i.e., <75th percentile) is enhanced by positive SST anomalies over the tropical North Atlantic and Mediterranean while heavy and extreme daily rainfall (i.e., >75th and >95th percentiles, respectively) are linked to El Niño–Southern Oscillation (ENSO) and interannual variability of Mediterranean SST. Their study, focused on the last 30 years, has shown that

Corresponding author: Aïssatou Badji, aissatou11.badji@ucad.edu.sn

DOI: 10.1175/JCLI-D-21-0699.1

warm SSTs over the tropical North Atlantic lead to enhanced low-level atmospheric instability over the Sahel. Superimposed on increased low-level moisture advection toward the Sahel from the equatorial and northern tropical Atlantic, this creates favorable conditions for the formation of horizontal stratiform clouds and, hence, moderate rainfall events. In contrast, extreme rainfall events are controlled by upper-level instability and convective precipitation systems. Such a mechanism is consistent with ENSO's remote influence. These results suggest that the climatic variability of the West African summer monsoon is more subtle than what has been described so far.

Furthermore, numerous studies based on daily rainfall data across Africa have analyzed the trends in rainfall characteristics over the last few decades. Focusing on the Sahel, Le Barbé and Lebel (1997) and Le Barbé et al. (2002) have shown that the rainfall deficit in the 1970–90 period is linked to a significant decrease in the frequency of rainfall events rather than intensity, particularly for extreme rainfall events (Panthou et al. 2013; Panthou et al. 2014). Sanogo et al. (2015) have shown that the average rainfall recovery in the Sahel over the last decades is reflected both in more rainy days and more extreme rainfall events. Sarr (2011) and Ly et al. (2013) have shown that extreme rainfall events have become more frequent in the Sahel over the 2001–10 decade, compared to 1961–90. However, and as shown by Lebel and Ali (2009), the recovery trend is not uniform over the Sahel: over the 1990–2007 period, both the central (11°–16°N, 10°W–0°E) and eastern Sahel (11°–16°N, 0°–10°E) are experiencing rainfall recovery while the western Sahel (11°–16°N, 20°–10°W) is still dry. Panthou et al. (2014) have shown that over the decade 2001–10, the central Sahel rainfall regime is characterized by a significant persistent deficit of rainfall occurrence compared to 1950–69, while at the same time the occurrence of extreme rainfall has strongly increased. Blanchet et al. (2018) have recently shown an increase in extreme daily rainfall over both the central and western Sahel since the 1980s, whereas Panthou et al. (2018) noticed that the eastern Sahel is experiencing a stronger increase in extreme rainfall compared to the western Sahel.

At the subregional scale, Hountondji et al. (2011) have studied the trend in extreme rainfall events in Benin (1960–2000). They showed a significant decrease in the annual total rainfall while extreme rainfall was relatively constant. New et al. (2006) have described a situation more prone to increases in extreme rainfall in Nigeria and over western Niger (Ozer and Ozer 2005), or the opposite in Guinea Conakry (Aguilar et al. 2009) and eastern Niger (Ozer et al. 2009). Lodoun et al. (2013) have shown a positive trend in the evolution of the annual rainfall, the number of rainy days, the daily rainfall intensity, and the onset and cessation dates of the rainy season in Burkina Faso since the end of the 1980s. Longueville et al. (2016) also showed a trend towards a recovery of rainfall in the same country in recent years. Over Senegal, using 1950–2007 daily precipitation data from 31 stations, Sarr et al. (2015) have shown a significant negative trend in the annual mean precipitation, the frequency of rainy days, the intensity of rainy days, and the 90th percentile of rain-day precipitation.

Despite the above mentioned studies on the trends of rainfall characteristics and their variability at interannual time scales, the decadal variability of rainfall characteristics in Senegal remains poorly documented in the literature. In this work we take advantage of a century-long record of daily rainfall data collected in different stations across Senegal to study the decadal variability of such rainfall characteristics and the potential sources thereof. Such a long record increases the robustness of the analysis by allowing the sampling of more events and providing results that are less dependent on a specific period.

To this aim, the paper is structured as follows: Section 2 describes the different datasets used, particularly the daily rainfall data and the methods used to evaluate its variability. Section 3 presents an analysis of the daily rainfall data, in particular verifying the homogeneity of the data and the spatial distribution of the time average of rainfall indices. Section 4 is centered on the analysis of the decadal variability of rainfall characteristics, their links with SSTs, and associated atmospheric mechanisms. Section 5 proposes conclusions.

2. Data and methods

a. General presentation of the data

This study is based on a century-long dataset of daily rainfall collected at different stations over Senegal. Senegal is located at the western tip of West Africa between longitudes 11.5°–17.5°W and latitudes 12°–16.5°N. The daily rainfall data are provided by the Regional Centre for the Improvement of Plant Adaptation to Drought [Centre d'Etude Régional pour l'Amélioration de l'Adaptation à la Sécheresse (CERAAS)]. The dataset includes daily rainfall records from the network of the former National Meteorological Agency in Senegal [now Agence Nationale de l'aviation Civile et de la Météorologie du Sénégal (ANACIM)] and other rain gauges managed by the Senegalese Institute for agricultural research [Institut Sénégalais de la Recherche Agricole (ISRA)]. The data have been collected at 143 stations in Senegal over the period 1900–2014. The stations are spread across the entire Senegalese territory (Fig 1b), with a greater density in the western region and along the north and western borders, which lies along the Senegal River [additional information about the data can be found in Salack et al. (2011)]. However, the data are sometimes not complete over the entire time period. A detailed analysis of this database and the pre-processing it has required is presented in section 3.

For validation purposes, the gridded monthly rainfall data from the Climatic Research Unit (CRU) TS version 4.04 are used. The CRUTS4.04 dataset spans from 1901 to 2019 at 0.5° × 0.5° spatial resolution (Harris et al. 2020). In addition, we have defined a CRU* subdataset defined as the CRU monthly rainfall at the closest CRUTS4.04 grid points to the stations.

Gridded monthly SST, sea level pressure (SLP), and land surface temperature (LST) data are also used to study the

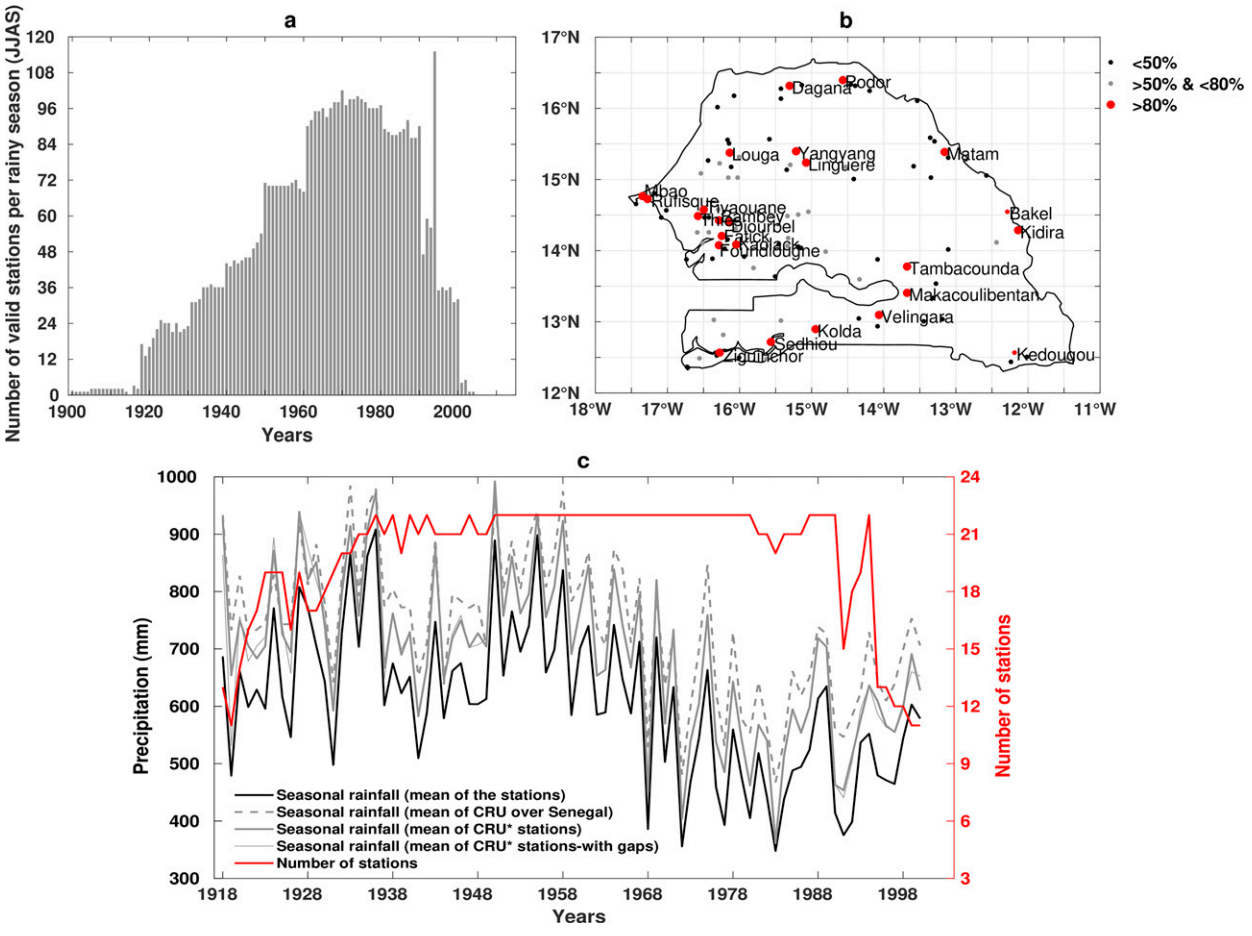

FIG. 1. (a) Number of valid stations per rainy season (JJAS) over the period 1900–2014 in Senegal. A station is considered valid if it has recorded more than 80% of daily data over the season. (b) Location of stations recording daily precipitation data in Senegal over the period 1918–2000. Stations where less than 50% of the total possible daily data have been recorded are represented with a black dot, stations where more than 50% and less than 80% of the total possible daily data have been recorded are represented with a gray dot, and stations where more than 80% of the total possible daily data have been recorded are represented with a red dot. The 22 homogeneous stations used in this study are shown with big red dots; the two non-homogeneous ones are in small red dots. The grid shows the CRU grill cells over Senegal. (c) Average seasonal amount of rainfall over the period 1918–2000 in Senegal. The black curve presents the average from the 22 homogeneous stations; the thick gray curve presents the average from the same 22 stations extracted from CRU*; the thin gray curve presents the average from the same 22 stations extracted from CRU* with gaps (see text for details); the gray dashed curve presents the average from CRU over the entire country of Senegal; and the number of stations is represented by the red curve corresponding to the axis on the right.

mechanisms explaining the changes highlighted by the above-mentioned daily rainfall data. SST data are taken from the Hadley Sea Ice and Sea Surface Temperature (HadISST) dataset. These are monthly reconstructions of SST provided by the Met Office Hadley Center. The HadISST data have a horizontal grid of 1° longitude × 1° latitude and span from 1870 to present (Rayner et al. 2003). Monthly SLP data are also taken from the Met Office Hadley Centre (HadSLP2). The HadSLP2 data are based on numerous compilations of land and marine pressure observations on a 5° latitude–longitude grid from 1850 to 2004 (Allan and Ansell 2006). Note however that the amount of data is lower over most of the tropical Pacific and Indian Oceans for a great part of the first half of the twentieth century (Allan and Ansell 2006). LST data are from Berkeley Earth Surface Temperature (BEST) dataset at 1° × 1° latitude–longitude grid spanning from 1750 to the present (Rohde et al. 2013).

b. *Statistical methods*

The statistical significance of the correlations obtained is estimated using the Ebisuzaki (1997) non-parametric test, which takes into account non-Gaussian and serially correlated data.

An empirical orthogonal function (EOF) analysis is also used. It is based on the recursively subtracted EOF (RSEOF) methodology. The RSEOF approach is particularly appropriate to EOF computations with datasets containing gappy data. It includes a compromise between accuracy and fast computation (Taylor et al. 2013). The RSEOF involves the

diagonalization of the covariance matrix of rainfall indices anomalies following a recursive procedure. At each iteration, only the leading EOF mode is retained, and the dataset is prepared for the next iteration by subtraction of that leading EOF. In this work, the rainfall indices anomalies are not standardized before computation of the EOFs.

Decadal modulations of rainfall indices are assessed from low-pass frequency filtering the time series using a Lanczos filter with a 13-yr cutoff period and 100 coefficients. Time series are filtered after EOF analysis.

SST, LST, SLP, and monthly rainfall data are extracted over the period 1918–2000. Annual anomalies of SST and summer (June–September) anomalies of LST, SLP, and monthly rainfall fields are calculated at each grid point, by subtracting climatology prior to detrending. We used the annual SST anomalies as the low-frequency variability of Sahel rainfall was reminiscent of the AMV and we were aiming at evaluating the low-frequency effect of the ocean.

3. Analysis of the daily database of Senegalese rainfall

a. Quality control and data homogeneity assessment

The first processing step of the daily rainfall series of the 143 stations is quality control. First, we removed unrealistic rainfall values (such as negative ones). Then, we quantified the yearly percentage of available daily data at each station over the period running from June to September (JJAS), with respect to the 122 days of the selected period. The period JJAS is selected here as it covers the monsoon rainy season of Senegal (e.g., Fall et al. 2006). The number of stations recording more than 80% of data per rainy season (JJAS) from 1900 to 2014 is very small or even zero before 1918 and after 2000 (Fig. 1a). We identified and isolated only 24 stations that have more than 80% of available data over the entire 1918–2000 period (red dots in Fig. 1b). Data from the 119 other stations (black and gray dots) are not further considered in this study.

The time series from the 24 pre-selected stations are then subjected to a homogeneity test. This step is needed to spot potential artificial changes in a station (such as a displacement of the station or modification of the instrument) that could have significantly impacted observations and thereby the record. We use the Alexandersson (1986) homogeneity test, based on the comparison of the record from the station being tested (test station) with surrounding stations (reference stations). It is a relative homogeneity test that assumes invariance along time of the normalized ratio between precipitation values at the test station and those defined as a weighted mean of precipitations from the reference stations.

In this work the reference stations are selected as those most correlated with the test station over the entire 1918–2014 period. In general, this corresponds to the closest stations. The weight given to each station is the square of its correlation coefficient with the test station. Such a homogeneity test has been applied to annual rainfall series in Alexandersson (1986) and monthly rainfall series in González-Rouco et al. (2001). We applied this test to the seasonal amount of rainfall at each of the 24 pre-selected stations. Our assumption is that nonclimatic abrupt or gradual changes introducing discontinuities or inhomogeneities (Ribeiro et al. 2016) in a station record should be reflected in the time series of the seasonal amount of rainfall. The seasonal amount of rainfall is calculated here for each station, by considering only daily rainfall from the JJAS seasons that have more than 80% of available data. That is, a JJAS season having less than 80% of available data (or with no rain) is considered as a season with no data recorded. Conclusions are insensitive to the choice of this threshold, as similar results are obtained using 85% or 90% thresholds (not shown). We varied the number of reference stations between one and three. We limited the number of reference stations to three so as to avoid considering very distant stations or stations with very small correlations. Yet, it is important to consider several stations in case the closest one is itself heterogeneous. In parallel, we applied the same test by considering for the reference the seasonal amount of rainfall from the CRU* series taken at the location of the test station. Therefore, we applied the homogeneity test four times for each test station. First, the data of the test station are compared with the reference station. Second and third, they are compared with the weighted mean of precipitation of first two and then three reference stations. Fourth, the data from the test station are tested against those in the CRU* grid cell to which the station belongs. The last test is an alternative to the assessment of the homogeneity of stations that are isolated or very far from others (e.g., Matam and Kedougou). In such cases indeed, even the "most correlated stations" can be only weakly correlated. In addition, certain stations fall into the same CRU* grill cell. This is the case for Foundiougne, Kaolack, Fatick, Diourbel, and Bambey; for Mbao and Rufisque; and finally for Linguere and Yangyang. Note that this latter test can also be seen as a safety test in the case where instrumentation changed simultaneously in all stations.

The results of the homogeneity test are reported in Table 1. A station is considered as inhomogeneous when all four tests performed result in a positive outcome (indicating heterogeneous behavior; labeled "n" in Table 1) and homogeneous (labeled "H" in Table 1) otherwise. Results show that 18 stations are initially homogeneous (names in bold), while six stations present inhomogeneities. A second step of the homogeneity test consists in attempting to correct the record, that is, to remove inhomogeneities in the stations. For this, the data of the years (over JJAS seasons) showing inhomogeneities are set to missing values (identified years given in the last column of Table 1). Thus, the four tests are applied again after this first "correction." Four stations (Dagana, Yangyang, Linguere, and Velingara) become homogeneous after correction, and two stations (Bakel and Kedougou) remain inhomogeneous (in italics). The inhomogeneities in these two stations could be explained by the fact that they are located in very remote and less supervised areas. Thus, they are more exposed to changes in the local environment. These two stations are not further used in this study.

Once the temporal homogeneity of the individual stations has been evaluated, we analyzed the spatial distribution of

TABLE 1. Stations subjected to the homogeneity test: H indicates homogeneous; HC indicates homogeneous after "correction"; n indicates non-homogeneous. See text for details.

Test stations	No. of reference stations			CRU* station	Years for which data were set to missing values to reach the homogeneity test
	1	2	3		
Mbao	H	n	H	n	—
Rufisque	H	H	H	H	—
Thies	H	n	H	H	—
Tivaoane	H	H	H	H	—
Foundiougne	H	H	H	H	—
Bambey	H	H	H	H	—
Ziguinchor	H	n	n	H	—
Fatick	H	H	H	H	—
Diourbel	H	n	n	H	—
Louga	H	H	H	H	—
Kaolack	H	H	H	H	—
Sedhiou	H	H	H	n	—
Dagana	HC	HC	HC	n	1933, 1996, 1997
Yangyang	HC	n	n	n	1945
Linguere	n	n	n	HC	1946, 1978
Kolda	n	n	n	H	—
Podor	n	n	n	H	—
Velingara	n	n	n	HC	1934
Makacoulibentan	n	n	n	H	—
Tambacounda	n	n	H	H	—
Matam	n	n	n	H	—
Bakel	n	n	n	n	1967, 1984
Kedougou	n	n	n	n	1926, 1954, 1995, 1996
Kidira	n	H	H	n	—

the remaining 22 stations. In Fig. 1c, we present the yearly seasonal amount of rainfall (thick black line) as well as the number of available stations per rainy season (JJAS) for each year (red line) from 1918 to 2000. The beginning and the end of the period are covered by fewer stations. In order to check the impact of this reduced number on the detected modulation of the seasonal rainfall amount, the average seasonal amount of rainfall obtained from the 22 homogeneous stations is compared to the CRU* 22 homogeneous stations, the CRU* 22 homogeneous stations including seasonal missing values, and the full regional CRU rainfall over Senegal. The missing stations during the beginning and the end of the study period are mainly located in the south of Senegal (not shown). This results, on the one hand, in a slight underestimation of the average seasonal amount of rainfall during these two periods, visible in the comparison of the complete CRU* time series (thick gray) with the one including the missing stations (light gray). This is consistent with the fact that there is on average less rainfall in the north of Senegal than in the south (Salack et al. 2014). Nevertheless, the analysis of the CRU* data shows that this underestimation is relatively weak and does not impact the decadal modulation of the seasonal amount of rainfall (Fig. 1c). The mean seasonal amount of rainfall over Senegal obtained from the average of stations (thick black line) is also underestimated as compared to the average of CRU over the entire Senegal (dotted gray line) (Fig. 1c). But again, this underestimation does not concern the variability since both time series are significantly correlated to 0.96 at the 95% level.

b. *Rainfall indices*

A set of rainfall indices is used to study the decadal variability of rainfall characteristics in Senegal (Table 2). Most indices are defined by the Expert Team on Climate Change Detection and Indices (ETCCDI), supported by the World Meteorological Organization (WMO) Commission for Climatology, the Joint Commission for Oceanography and Marine Meteorology (JCOMM), and the Research Program on Climate Variability and Predictability (CLIVAR) and have used in previous studies (e.g., Sillmann et al. 2013; Sanogo et al. 2015; Diakhate et al. 2019). Those indices are the number of dry days (NDD), the number of rainy days (R1mm), the simple daily intensity index (SDII), the number of heavy precipitation days (R10mm), the number of very heavy precipitation days (R20mm), the number of wet days with rainfall above the 75th percentile (R75p), and the number of very wet days (R95p). A dry day is defined as a day with less than 1 mm of rainfall. A rainy day is defined as a day recording at least 1 mm of rainfall. The SDII index is calculated as the average rainfall from rainy days. The R10mm and R20mm indices correspond to the number of days with daily rainfall exceeding 10 and 20 mm respectively. The R75p and R95p indices correspond to the number of days with daily rainfall exceeding the 75th and 95th percentiles of rainfall of rainy days, respectively. The 75th and 95th percentile

TABLE 2. Definition of the rainfall indices used in this study. I: Rainfall indices based on ETCCDI definitions. II: Rainfall indices based on Sivakumar's (1988) and Marteau's (2010) definitions.

Group	Abbreviation	Definition	Unit
I	TOTSR	Seasonal amount of rainfall	mm
	NDD	Seasonal number of days when daily rainfall is less than 1 mm	days
	R1mm	Seasonal number of days when daily rainfall is at least 1 mm	days
	SDII	Total seasonal rainfall divided by the cumulated number of rainy days in the season	mm day^{-1}
	R10mm	Seasonal number of days with daily precipitation above 10 mm	days
	R20mm	Seasonal number of days with daily precipitation above 20 mm	days
	R75p	Seasonal number of days with rainfall amount above the 75th days percentile of rainfall of rainy days	days
	R95p	Seasonal number of days with rainfall amount above the 95th days percentile of rainfall of rainy days	days
II	SDrs	Onset date of the rainy season	day
	EDrs	Cessation date of the rainy season	day
	Lrs	Length of the rainy season	days

thresholds are defined locally at each station. We computed all these indices from the daily record of the 22 homogeneous stations focusing over the rainy season (JJAS) in Senegal. The seasonal amount of rainfall (TOTSR) over Senegal is used here for comparison with the other indices and previous works.

Additional indices are also defined in order to characterize the rainy season temporally. These are the onset date, cessation date, and the length of the rainy season. There are various definitions of the onset and cessation dates of the rainy season in the literature (e.g. Sivakumar 1988; Marteau et al. 2009; Marteau 2010; Liebmann et al. 2012; Dunning et al. 2016). Sivakumar (1988) and Marteau (2010) for example have used definitions tuned to capture onset and cessation dates of the rainy season over West Africa specifically, whereas Liebmann et al. (2012) and Dunning et al. (2016) used onset and cessation date definitions valid over all of Africa. In this study, we only compared the two regional definitions [i.e., those of Sivakumar (1988) and Marteau (2010)] to assess the onset and cessation dates of the rainy season in Senegal and the uncertainty coming from these definitions. According to Sivakumar (1988), the onset date of the rainy season in the Sahelian and Sudanese regions is the date after 1 May when at least 20 mm of rainfall has been collected over 3 consecutive days, with no dry sequences of more than 7 consecutive dry days during the following 30 days. The cessation date of the rainy season is the date after 1 September following which no rain occurs over a period of 20 days. Here, the onset date and the cessation date are calculated over the periods from May to August (MJJA) and from September to November (SON), respectively. As for the former indices, only MJJA and SON periods having more than 80% of available data are considered. The length of the rainy season is the difference in days between the cessation date and the onset date. Note that therefore, as stated above, there is no unanimous definition of the onset and cessation dates of the rainy season over West Africa and thus results are, to some degree, dependent on the chosen definition. As an estimate of the uncertainty arising from this definition, we also evaluated the indices related to the timing of the rainy season based on the criterion provided by Marteau (2010), slightly modified here to account for missing data: the onset date is the date of the first rainy day of a sequence of 4 consecutive days cumulating at least 20 mm, with no dry sequences of more than 10 consecutive dry days during the following 20 days. The cessation date is defined as the date of the last day (+1) of the last sequence of 4 consecutive days accumulating at least 20 mm, with no dry sequences of more than 10 consecutive dry days in the previous 20 days. The main difference here with Marteau's (2010) definition is that in both cases, the sequence of 4 consecutive days is not necessarily "wet." This criterion is thus less restrictive but more adapted to the very sparse rainfall events on the north of Senegal. These somewhat different definitions yield earlier onset and cessation dates across Senegal than those based on Sivakumar (1988) (not shown).

In the following, only results from Sivakumar's (1988) definitions will be shown and a comparison of results from the two methods will be discussed in the conclusions (section 5).

All the rainfall indices are computed at each station separately. The calculation for all of Senegal is done by taking the average of stations for each year. That is, for a given year and a given index, we take the sum of the values computed at each individual station divided by the number of available stations for a specific year.

c. *Spatial distribution of the time-mean values of the rainfall indices*

The time average of each index and for each station is calculated over the period 1918–2000 so as to give a general view on the spatial distribution of these quantities. The highest seasonal amounts of rainfall (TOTSR) are observed in southern Senegal with more than 800 mm per rainy season (Fig. 2a). In northern Senegal, the mean values of TOTSR are less than 400 mm per year. Similar results have been shown by Salack et al. (2014) over Senegal, using the same daily rainfall database but focusing on the period 1950–2010. Because of this shorter period of study, they have been able to use daily rainfall data from 31 stations over Senegal. The mean number of dry days (NDD), number of rainy days (R1mm), and intensity

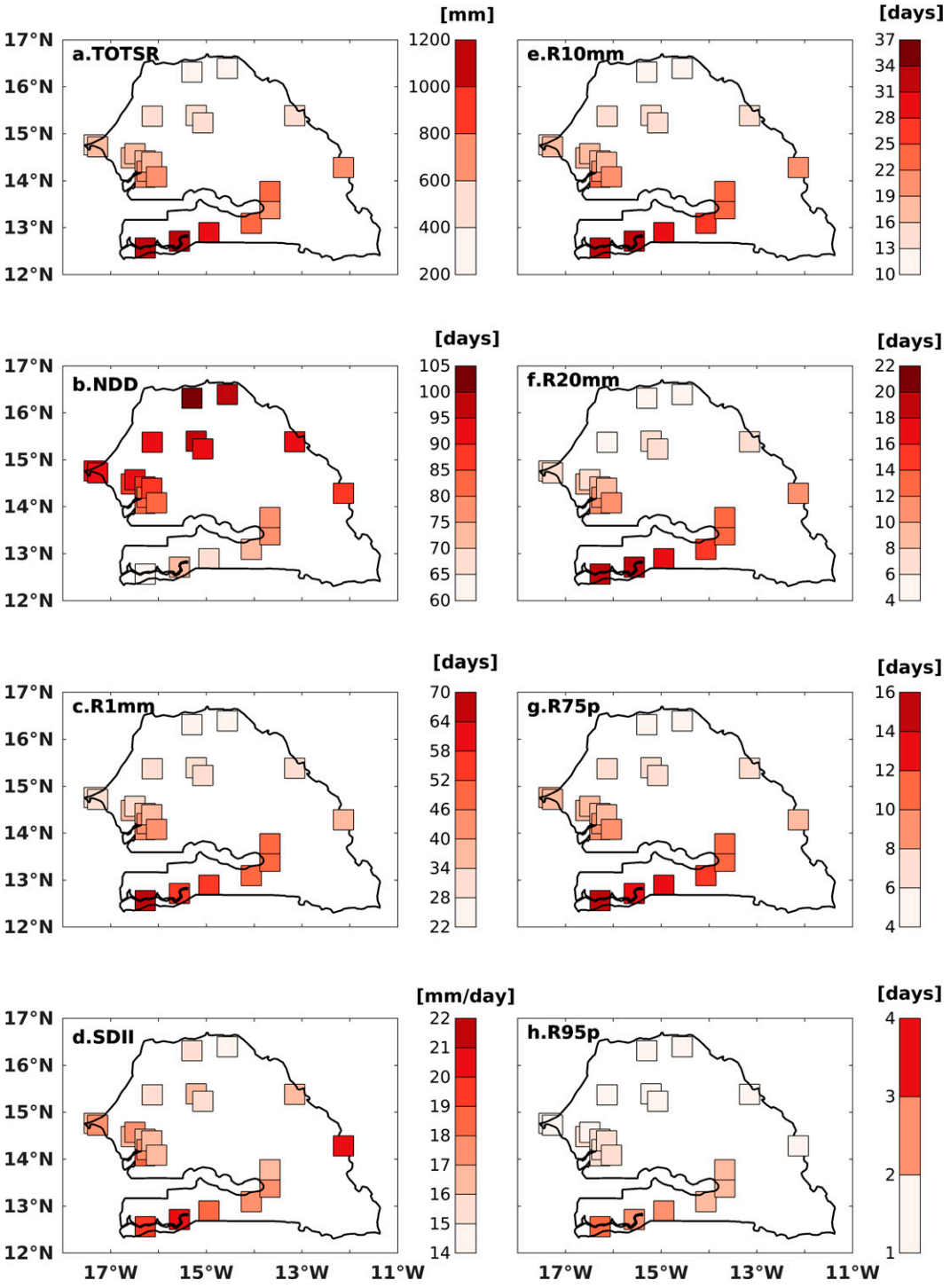

FIG. 2. Spatial distribution of the mean values of (a) TOTSR, (b) NDD, (c) R1mm, (d) SDII, (e) R10mm, (f) R20mm, (g) R75p, and (h) R95p rainfall indices computed over the period 1918–2000 for each station.

of rainfall events (SDII) are shown in Figs. 2b–d. The mean frequency of daily rainfall exceeding 10 and 20 mm (i.e., R10mm and R20mm) and frequency of daily rainfall above the 75th and 95th percentiles of rainfall of rainy days (i.e., R75p and R95p) are shown in Figs. 2e–h. Figures 2c, 2e, and 2f show that the mean values of R1mm, R10mm, and R20mm are greater in the south than in the north of Senegal. We note on average more than 50 days of R1mm, 30 days of R10mm, and 20 days of R20mm per year in the south against less than 30 days of R1mm, 15 days of R10mm, and 10 days of R20mm per year in

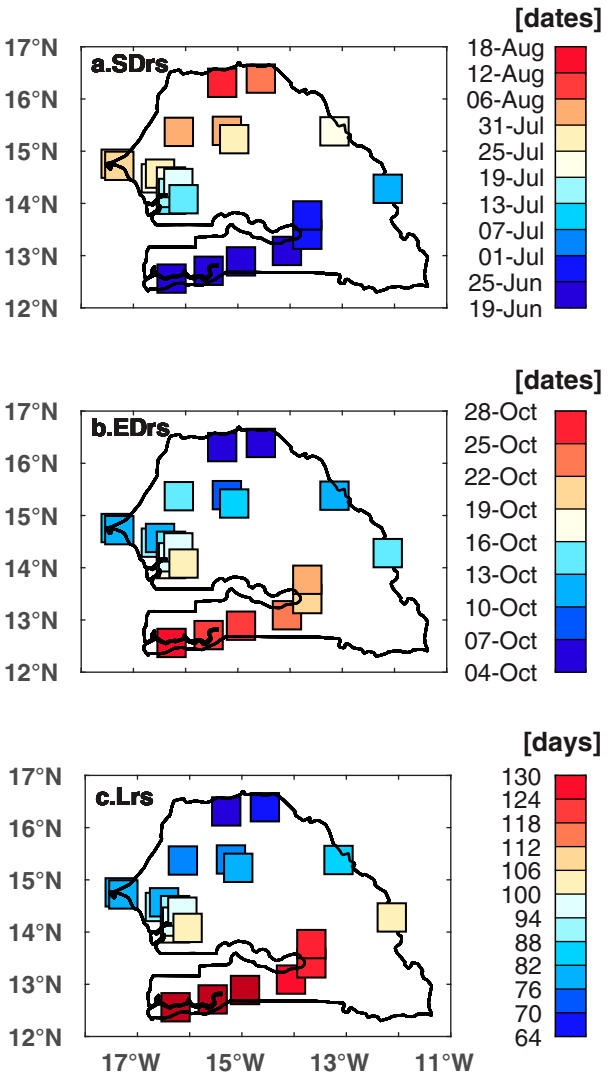

FIG. 3. As in Fig. 2, but for (a) SDrs, (b) EDrs, and (c) Lrs indices.

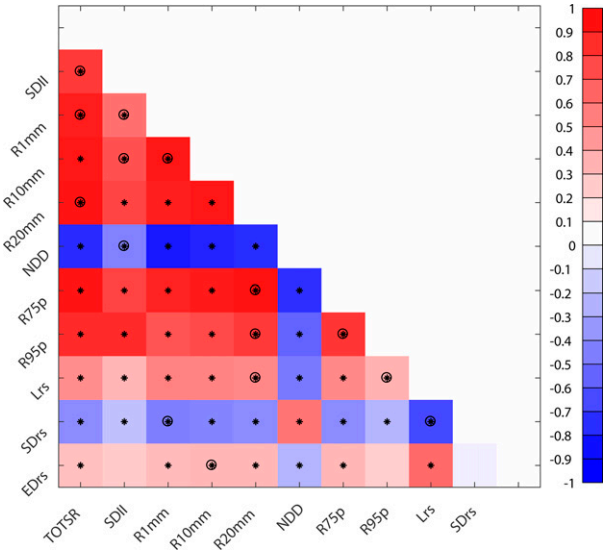

FIG. 4. In-phase correlation coefficients between the regionally averaged rainfall indices (colors). Asterisks indicate correlations significant at the 95% confidence level. Circles indicate that 17 of the 22 correlations among the same indices computed for each station individually are significant at the 95% level.

the north. The mean values of R75p and R95p also show spatial distributions characterized by values 4 times stronger in the south of Senegal compared to the north (Figs. 2g,h). The mean values of SDII are also higher in the south of Senegal compared to the north (Fig. 2d). Conversely, the mean values of NDD are more pronounced in the north of Senegal where more than 95 dry days per year (still over JJAS season) are observed (Fig. 2b). Note that figures scaled in terms of percentage of the mean precipitation at the station located most southwestward (Ziguinchor) confirm that the north–south gradient is of similar amplitude for each frequency index (not shown).

Figure 3 shows the mean distributions of indices related to the timing of the rainy season (i.e., SDrs, EDrs, and Lrs). The mean onset (SDrs) and cessation (EDrs) dates of the rainy season are presented in terms of dates. As with the former indices, a meridional gradient is observed in the spatial distribution of SDrs and EDrs (Figs. 3a,b). Latest onset dates of the rainy season are found in the north of Senegal, where the monsoon can start as late as the end of July or the beginning of August. In the southern part of the country, the mean onset date is generally around the mid of June. The mean cessation date of the rainy season (EDrs) in the north is the beginning of October whereas it can reach the end of October in the south of Senegal. The meridional gradient of SDrs and EDrs has implications in terms of the length of the rainy season (Lrs). The average length of the season is less than 70 days in the north of Senegal while it can exceed 120 days in the south (Fig. 3c). These results are in agreement with Sivakumar (1992).

d. Temporal covariability of the rainfall indices

Prior to the analysis of the decadal variability of rainfall indices, we proceeded to an intercomparison of the indices defined above, in order to identify their temporal covariability. For this, we calculated their cross-correlations at each station separately as well as for the regionally averaged indices (Fig. 4). The TOTSR index is considered here as the reference. Figure 4 shows significant positive correlations between TOTSR and the R1mm, SDII, and R20mm indices in more than 17 out of the 22 stations as well as in terms of regional average. In addition, R10mm shows significant positive correlations with SDII, R1mm, and EDrs. R75p also shows significant positive correlations with R20mm and R95p. Lrs is significantly positively correlated with R20mm and R95p. Conversely, NDD is significantly negatively correlated with SDII. One can also note negative correlations between SDrs and almost all other indices. However, only the correlations with R1mm and Lrs are significant in more than 17 out of the 22 stations and in terms of regional average.

4. Spatiotemporal variability of Senegalese summer rainfall characteristics at decadal timescales

a. EOF analysis of rainfall characteristics

In order to analyze the decadal variability of the rainfall characteristics in Senegal, we performed an empirical orthogonal function (EOF) analysis, following the RSEOF approach described in section 2b applied to the raw interannual data. For all indices, the first EOF is significantly separated from the second one according to the North et al. (1982) rule of thumb, unlike the second and third ones. Therefore, only the first EOF and its associated principal component (PC) is considered here.

Figures 5 and 6 show the first EOF patterns and corresponding PCs of the seasonal amount of rainfall (TOTSR), the number of dry days (NDD), the number of rainy days (R1mm), the mean intensity of rainfall events (SDII), the number of heavy and very heavy daily rainfall events (i.e., R10mm and R20mm), and the number of daily rainfall events exceeding the 75th and 95th percentiles of rainfall of rainy days (i.e., R75p and R95p). In the following, for simplicity, R1mm and R10mm are named the frequency of light rainfall events, R20mm and R75p are named the frequency of heavy rainfall events and R95p is named the frequency of extreme rainfall events. Figure 7 shows the EOF patterns and corresponding PCs of indices related to the timing of the monsoon season (i.e., SDrs, EDrs, and Lrs). In Table 3, the percentages of variance explained by the EOFs of each rainfall indices are reported.

The first EOFs of the seasonal amount of rainfall, the light rainfall events, or the number of dry days explain around 50% of the total variance of each index respectively, whereas only 40% of the total variance is explained for the heavy rainfall events and 20% for the extreme rainfall events and the mean rainfall intensity. In the case of the monsoon timing (SDrs, Lrs, and EDrs), the explained variances of the first mode range from 30% to 40%.

Figures 5a1–d1, 6e1–h1, and 7a1–c1 show that the first EOF patterns of indices show anomalies with a uniform sign over the full domain, suggesting a uniform mode of variability over Senegal. Most indices nevertheless show a north-to-south increase in EOF loads, consistent with the mean values shown in Fig. 2. The index of mean rainfall intensity (SDII) rather shows high loads to the east. Yet the analysis of SDII removing the two easternmost stations shows that the time variability of the resulting EOF is unchanged, the two low-pass filtered PCs being significantly correlated to 0.88 at the 95% level (not shown). Another exception concerns those indices related to the timing of the monsoon season, which tend to show higher loads near the western coast. The PCs associated with the first EOFs of indices related to the timing of the monsoon season show less decadal-to-multidecadal variability than those related to the amplitude or frequency of rainfall events: the variance of the low-pass filtered PC with a cutoff period of 13 years is about 20% of that of the raw PC for the former ones while the corresponding ratio lies between 43% and 54% for the amplitude or frequency of rainfall events. The PC of the seasonal amount of rainfall shows that the decadal variability of TOTSR is characterized by a wet period from the 1930s to the 1950s, followed by a long dry period from the 1970s to the 1990s (Fig. 5a2). This decadal variability is consistent with the well-known monsoon variability of the entire Sahel region (e.g., Rowell et al. 1992; Giannini et al. 2003; Mohino et al. 2011a). The first PC of indices related to the intensity and frequency of rainfall events also shows a marked decadal variability (Figs. 5b2–d2 and 6e2–h2), which is close to that of TOTSR. This supports Biasutti's (2019) result concerning a strong link between the seasonal rainfall amount and frequency of rainy days over the Sahel during the second half of the twentieth century. The corresponding PCs of SDrs, EDrs, and Lrs also show decadal variability, but it is relatively weaker, as indicated above (Table 3, Figs. 7a2–c2). Note that the time evolution of all indices contains a strong linear trend that accounts for about half of the variance of each low-pass filtered index respectively (not shown).

b. Sources and mechanisms of decadal variability of frequency and intensity of rainfall events

As detailed in section 1, several studies have highlighted the role of North Atlantic SST modulations for the low-frequency variability of the seasonal amount of rainfall (TOTSR), in particular at the scale of Sahel (Giannini et al. 2003; Mohino et al. 2011a) but also of Senegal (Wade et al. 2015). To investigate the possible sources of the decadal variability of rainfall indices in Senegal, we computed the correlations of the low-pass filtered PCs of the indices characterizing the frequency of rainy events with the annual anomalies of SST. We also considered the summer (JJAS) anomalies of SLP, as well as the low-pass filtered (JJAS) anomalies of rainfall over the land to investigate possible teleconnection mechanisms. In addition, to identify associated land surface temperature (LST) changes, we calculated correlations of the low-pass filtered PCs of rainfall indices with the summer anomalies of LST. Note that the conclusions are insensitive to the choice of filtering of SST, LST, and SLP anomalies (not shown). To remove the influence of a possible centennial trend in the PCs and concentrate on decadal to multidecadal variability, all fields and time series have been linearly detrended prior to computations.

Figure 8 shows that an increase in TOTSR in Senegal is related to a large SST warming over the North Atlantic Ocean and the Mediterranean Sea and SST cooling over the tropical Indian and Pacific Oceans (Fig. 8a). Such SST pattern shows similarities with the AMV, and this is consistent with the previous studies cited above. The decadal variability of frequency and intensity of rainfall events is related to similar patterns of SST as for TOTSR albeit with some differences (Figs. 8b–h).

Over the North Atlantic, R1mm and, especially, NDD show less significant positive correlations with SST in the tropical and extratropical parts. This differs from R10mm and the heavy and extreme rainfall indices, which show patterns closer to that of the AMV (Figs. 8b,c,e–h). A possible explanation to this could be linked to the role of the Atlantic Ocean as a moisture source for Sahel rainfall (Nieto et al. 2006).

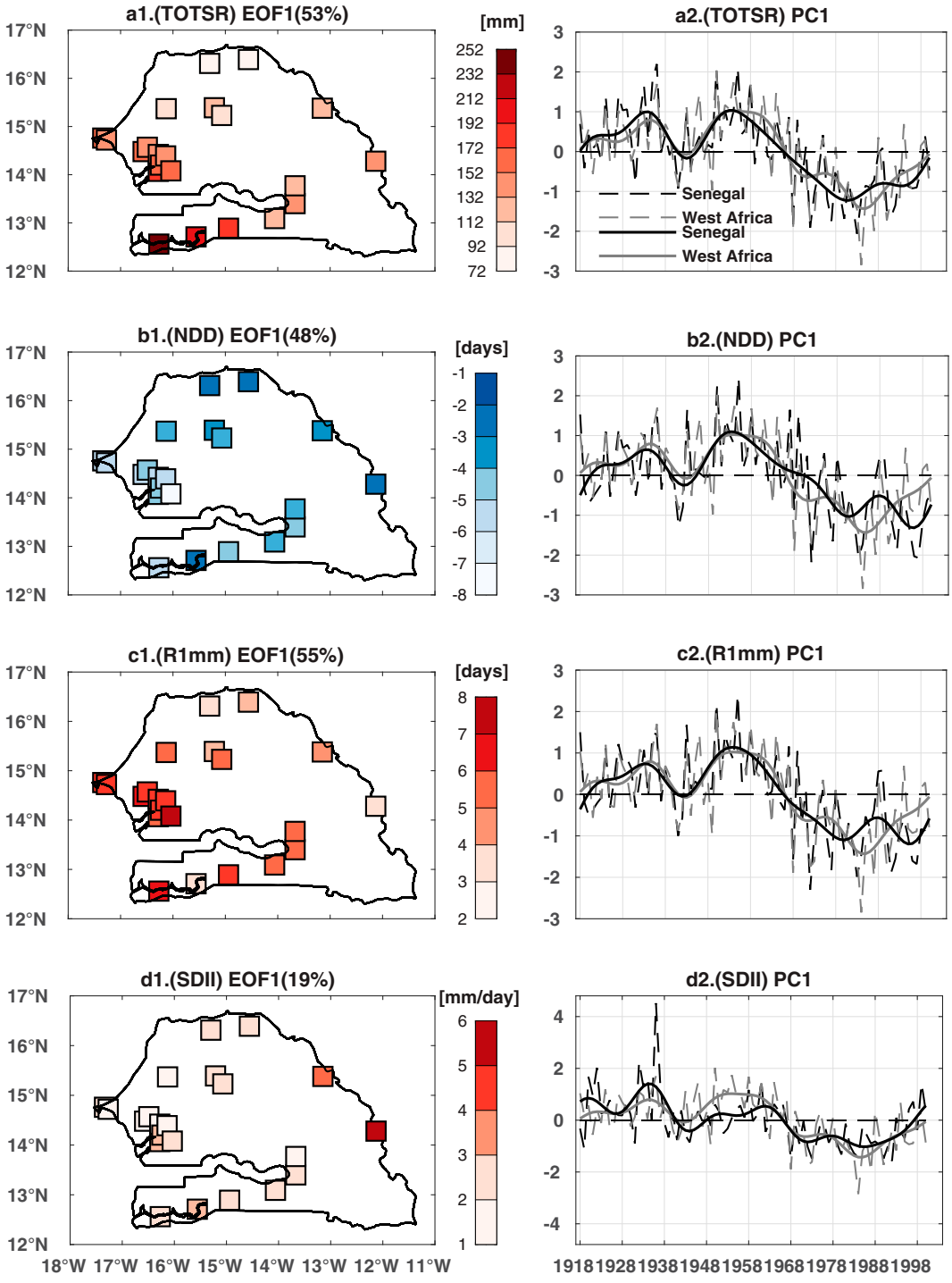

FIG. 5. Leading EOF anomalous patterns of (a1) TOTSR (mm), (b1) NDD (days), (c1) R1mm (days), and (d1) SDII (mm day^{-1}). The number inside the parentheses is the explained variance of the first EOF for each index. (a2)–(d2) The corresponding principal components of all indices are in black curves (standardized anomalies). The raw interannual PCs are the dotted curve. The solid black curves show the low-pass filtered time series (see text for details). The gray curve superimposed to the PCs of all indices corresponds to the leading principal component of the seasonal amount of rainfall over West Africa (0°–30°N, 20°W–10°E) computed from the CRU dataset. The PCs of all indices are normalized (no units).

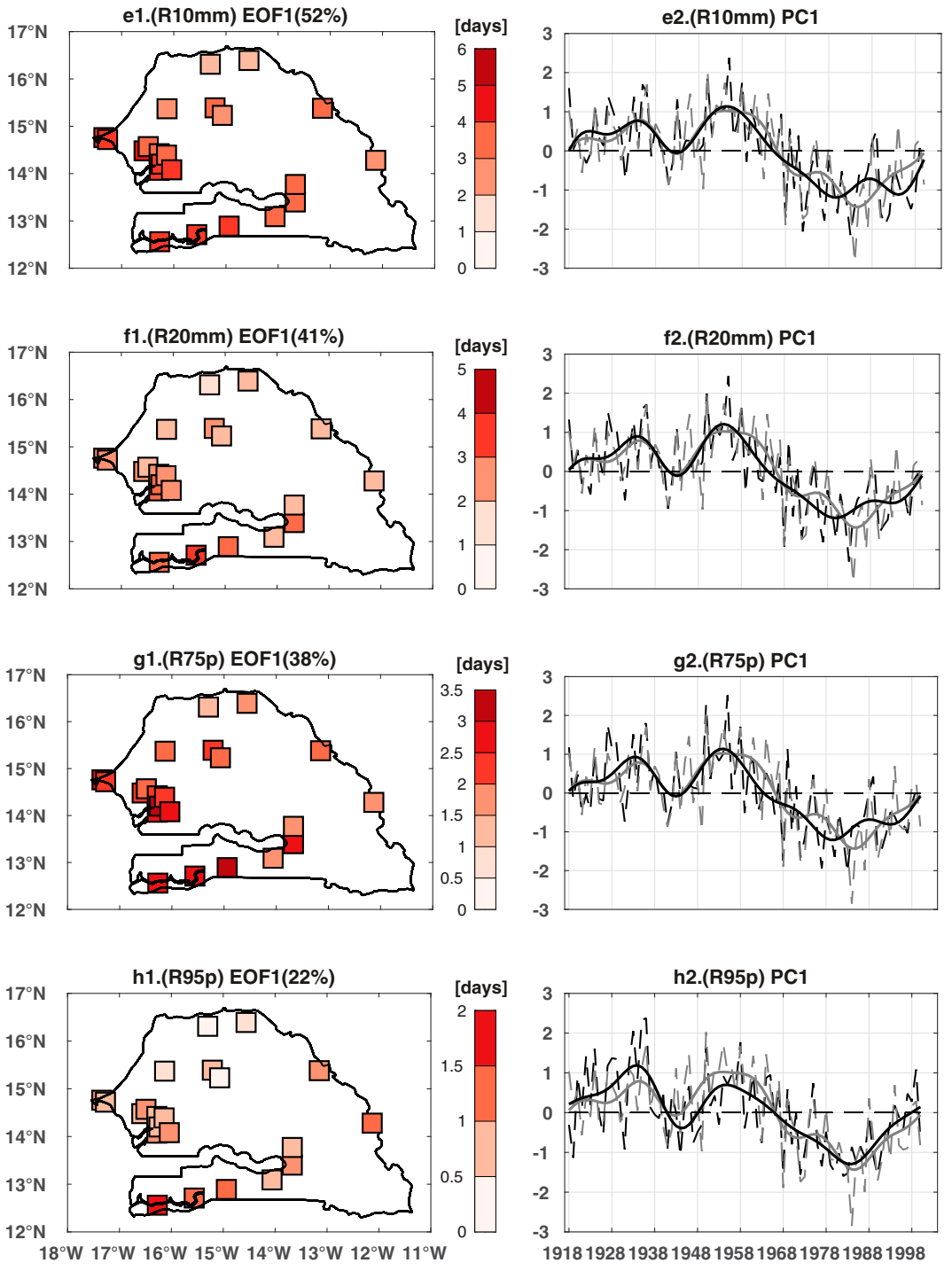

FIG. 6. As in Fig. 5, but for (e) R10mm (days), (f) R20mm (days), (g) R75p (days), and (h) R95p (days).

A warmer Atlantic can provide more moisture and enhance the occurrence of heavy and extreme rainfall (e.g., Giannini et al. 2013). R1mm and NDD are less concerned by this excess of moisture supply. The mean rainfall intensity (SDII) index shows a pattern much more centered in the central North Atlantic Ocean and barely significant along the coasts of North America and Europe (Fig. 8d). The exact reason for this difference is not clear, although it could be partly related to the lower spatial coherence that the variability of SDII shows over Senegal (Moron et al. 2006).

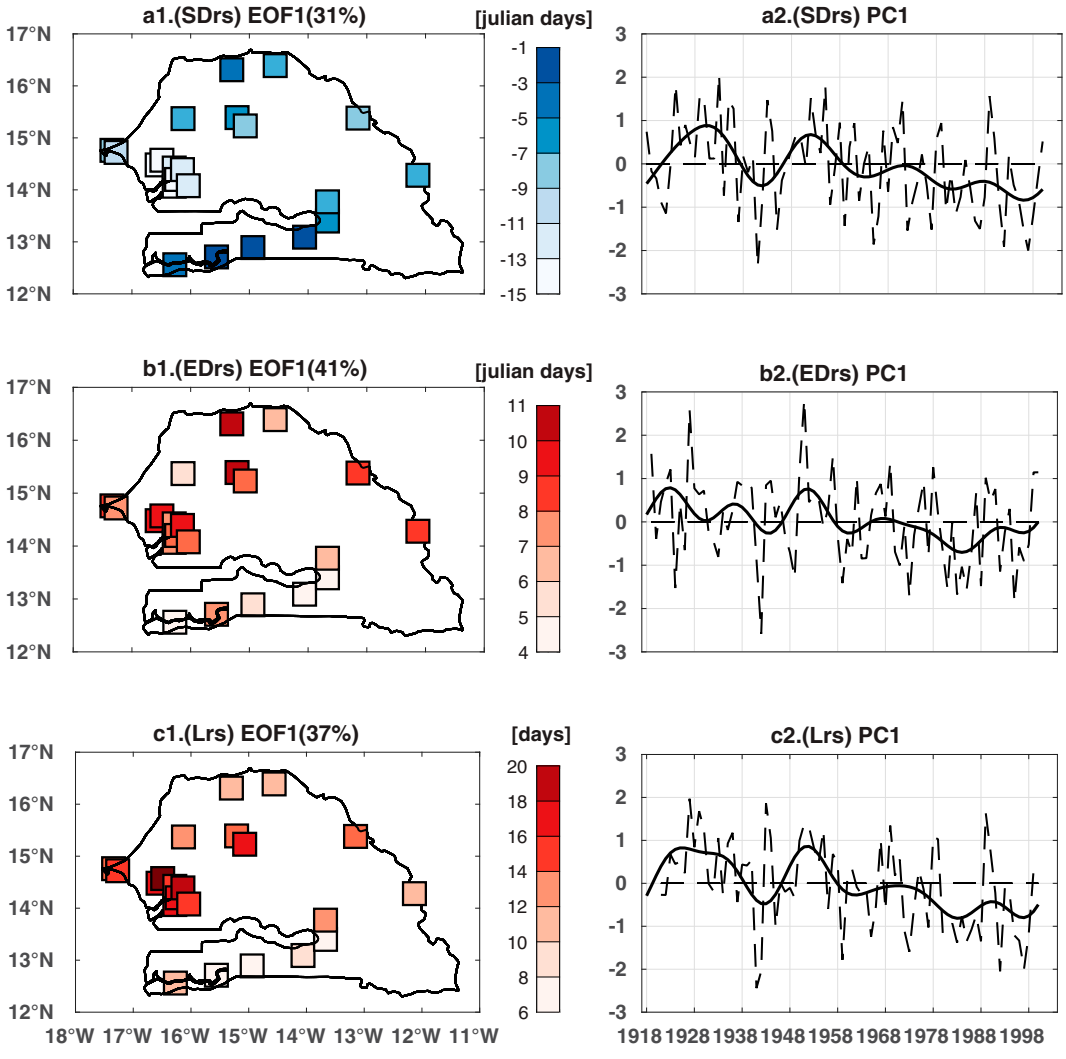

FIG. 7. As in Fig. 5, but for the (a) SDrs (Julian days), (b) EDrs (Julian days), and (c) Lrs (days) indices.

A decrease (increase) of NDD (R1mm) seems to be also related to SST warming over the western Mediterranean (Figs. 8b,c), while an increase of SDII and R95p seems to be more influenced by SST warming over the eastern Mediterranean (Figs. 8d,h). This relation of eastern Mediterranean SST and rainfall intensity, particularly for extreme events, could be connected to the eastern Mediterranean's role as an important provider of moisture for Sahel rainfall (Nieto et al. 2006). Warmer SSTs over the eastern Mediterranean could increase the overall moisture reaching the Sahel and, thus, the intensity of rainfall events.

Over the Indian and Pacific tropical oceans, SST cooling is associated with an increase of the frequency of light and heavy rainfall events in Senegal at decadal time scales (Figs. 8c,e,f,g). The relation between a decrease of the number of dry days (NDD) and a cooling over tropical Pacific and Indian Oceans is even stronger (Fig. 8b), while the Pacific seems to have no significant influence on the mean intensity

TABLE 3. Amount of total variance explained by the principal components of each index. The first row of each index indicates the total amount of variance explained by the raw PC. The second row indicates the amount of variance at the decadal timescale (i.e., variance of the low-pass filtered PC) entailed by each PC (ratio of the variance of the filtered time series to the variance of the unfiltered time series) for each index.

Rainfall indices	TOTSR	NDD	R1mm	SDII	R10mm	R20mm	R75p	R95p	SDrs	EDrs	Lrs
Variance explained by each PC (%)	53	48	55	19	52	41	38	22	31	41	37
Decadal variance of each PC (%)	54	43	51	45	53	53	49	47	22	14	27

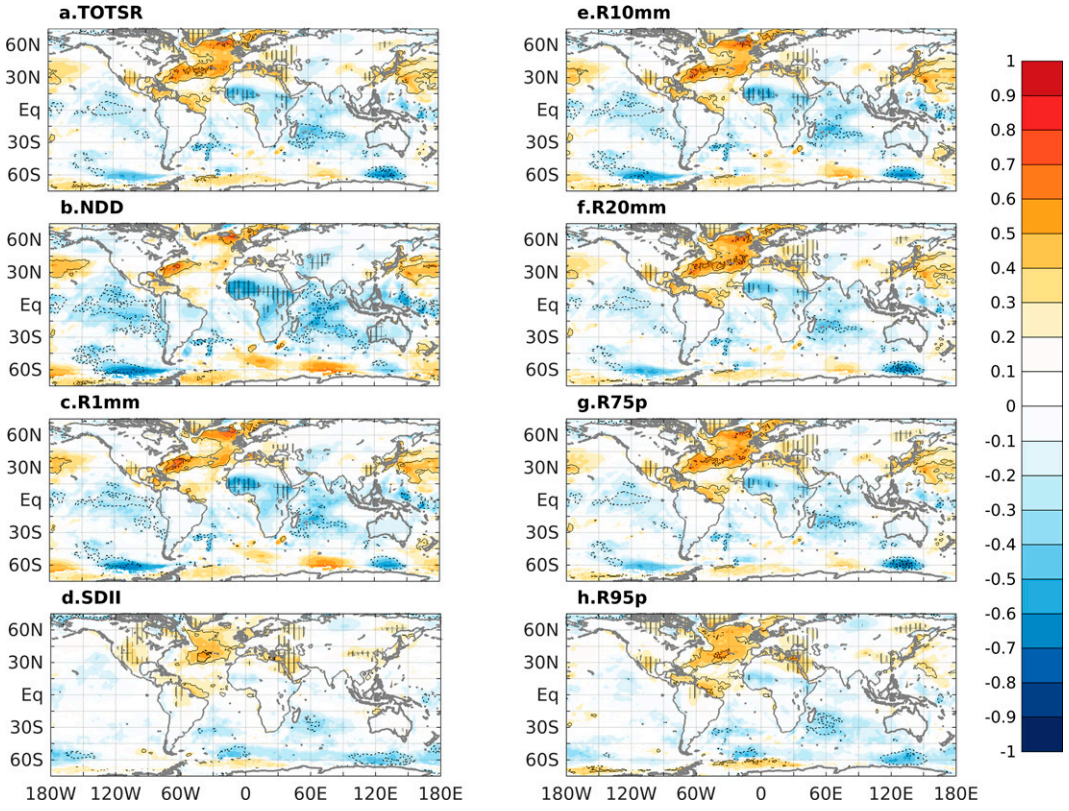

FIG. 8. Correlation maps of annual anomalies of SST over the ocean and JJAS anomalies LST over the continents with the low-pass filtered PCs of (a) TOTSR, (b) NDD, (c) R1mm, (d) SDII, (e) R10mm, (f) R20mm, (g) R75p, and (h) R95p rainfall indices. Contours (for SST) and stripes (for LST) indicate significant correlations at the 95% confidence level. The low-pass filtered PCs of indices as well as the SST and LST fields are all linearly detrended.

of rainfall (SDII) and on the extreme rainfall events (R95p) at these time scales (Figs. 8d,h). A possible explanation for the connection of the different rainfall indices with Indian and Pacific tropical SSTs could be that a warming of remote ocean basins warms the tropical upper troposphere over the Sahel, which increases the threshold for convection and reduces precipitation (Rowell 2001; Giannini et al. 2008; Giannini and Kaplan 2019).

An increase in TOTSR over Senegal is also associated with prominent low pressure anomalies over the tropical and midlatitude North Atlantic and the Mediterranean Sea (Fig. 9a). The low pressure anomalies over the North Atlantic and Mediterranean Sea are related to SST warming over both basins, consistent with the warm phase of AMV (Ruprich-Robert et al. 2017) and in agreement with Fig. 8a. During a warm AMV phase, SST warming over the North Atlantic and little to no SST cooling over the South Atlantic create an interhemispheric SST gradient reflected in an anomalous SLP gradient. This hemispheric differential warming creates an excess of energy input into the atmosphere in the Northern Hemisphere. In the equator, this excess is transported towards the south by the northward shift of the southern Hadley cell (e.g., Schneider et al. 2014; Biasutti et al. 2018). This northward shift of the Hadley cell is related to a northward shift of the intertropical convergence zone (ITCZ), and therefore an increase in rainfall over the Sahel (Folland et al. 1986; Rowell et al. 1995; Ward 1998; Knight et al. 2006; Zhang and Delworth 2006; Ting et al. 2009; Martin and Thorncroft 2013; Monerie et al. 2019) and a decrease of rainfall over northeastern Brazil (Knight et al. 2006) (Fig. 9a). The spatial coherence of the seasonal rainfall in the Sahel at decadal time scales is consistent with the results of Wade et al. (2015).

Moreover, a warmer eastern Mediterranean has been shown to lead to a farther northward migration of the West African monsoon system due to strengthened southwesterly flow (Rowell 2003; Fontaine et al. 2010, 2011) and weakened northeasterly wind (Peyrillé et al. 2007). An increase in rainfall in the Sahel is associated with low pressure anomalies over the eastern Mediterranean (Fig. 9a), in accordance with Raicich et al. (2003). Figure 9a also shows significant low pressure anomalies over western Europe and in the Caribbean related to the AMV warm phase, in agreement with previous findings from Sutton and Hodson (2005).

A similar general structure is observed for a decrease of NDD and for an increase of SDII, R1mm, R10mm, R20mm, R75p, and R95p (Figs. 9b–h). Nevertheless, for a decrease (increase) of NDD (SDII and R95p), the low pressure anomalies are much weaker in the extratropical North Atlantic (Figs. 9b,d,h), compared to the other indices. In addition, an increase of the seasonal amount of rainfall and the extreme

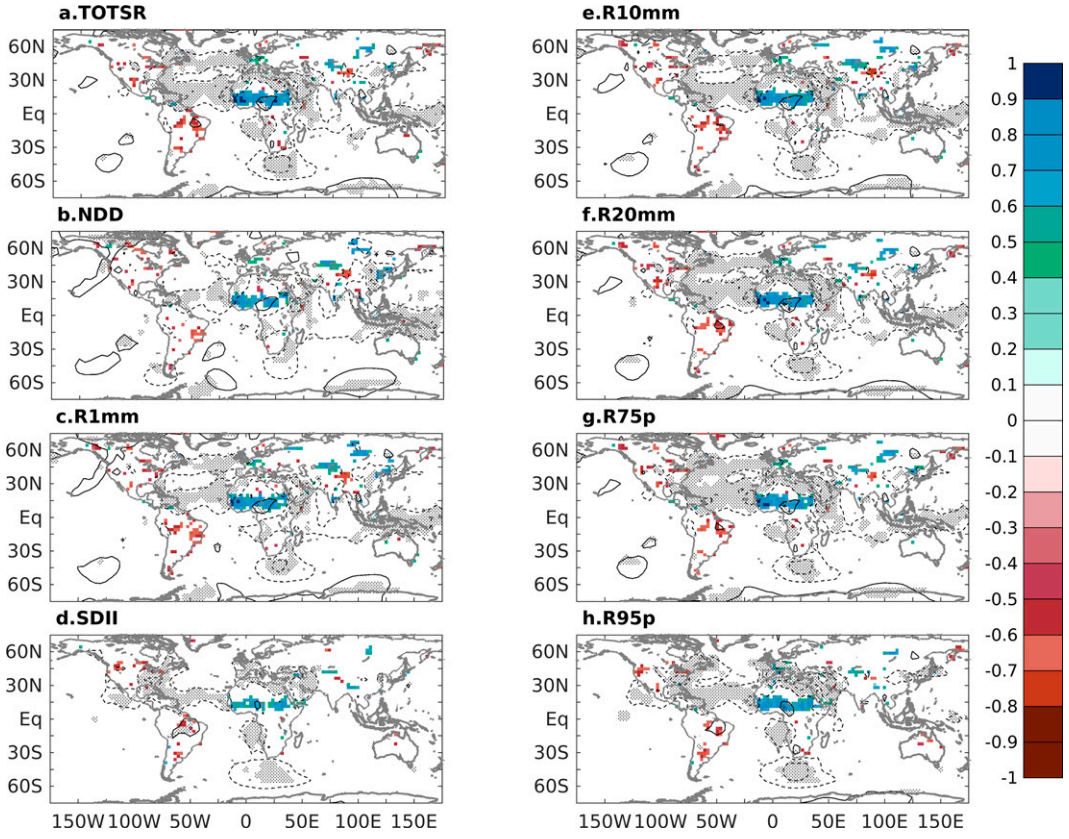

FIG. 9. Correlation maps of JJAS anomalies of SLP and the low-pass filtered (JJAS) anomalies of rainfall over the continents with low-pass filtered PCs of (a) TOTSR, (b) NDD, (c) R1mm, (d) SDII, (e) R10mm, (f) R20mm, (g) R75p, and (h) R95p rainfall indices. Colors are for rainfall (only shown where significant at the 95% confidence level) and contours are for SLP (negative values are in dashed contours and positive values are in solid contours; the contour interval is 0.2, and the zero contour is not shown; stippling indicates significant correlations at the 95% confidence level). The PCs of indices as well as the SLP and rainfall fields are all linearly detrended.

rainfall events over Senegal is associated with low pressure anomalies over the entire Mediterranean Sea (Figs. 9a,h), whereas for a decrease of the number of dry days and, especially, an increase of the mean intensity of rainfall events, the frequency of light and heavy rainfall events, the low pressure anomalies are restricted to the eastern Mediterranean only (Figs. 9b–g). Such connection of the intensity and extreme events occurrence to the eastern Mediterranean SLP anomalies with little to no role of the extratropical Atlantic SLP anomalies could be linked to the aforementioned role of this area as a source of humidity for Sahel rainfall, which, when warmer, could induce both an enhancement of moisture content ready for strong rainfall events and a reduction of Mediterranean SLP. Moreover, there are little to no significant correlations with the SLP over the Indian and Pacific tropical oceans (Figs. 9a–h), which could be due to the lack of available SLP data over those regions in the earlier record (Allan and Ansell 2006).

Regarding rainfall, all indices show significant positive correlations across the Sahel and negative ones over northeastern Brazil (Figs. 9b–h), which is consistent with the aforementioned northward shift of the Atlantic ITCZ as a response to the interhemispheric SST pattern. In addition, most indices show positive correlations with rainfall over central Europe, which is consistent with the overall AMV pattern obtained for SSTs in the North Atlantic (Knight et al. 2006). A notable exception is the SDII index, which also showed an SST pattern with little to no loads along the coasts of western Europe (Fig. 9d).

Correlations of the rainfall indices with surface temperatures are much less extended over land than over the ocean (Fig. 8). An increase in TOTSR in Senegal is accompanied by decreasing temperatures throughout the Sahel and in the highlands of Ethiopia (Fig.8a). Giannini et al. (2003) indeed showed that a positive rainfall anomaly in the Sahel leads to an increase of the soil moisture and a decrease of local land surface temperatures because the incident energy flux is used more to evaporate moisture rather than to heat the surface. In addition, a reduction in surface temperatures over these regions could also be associated with enhanced cloud cover and reduced shortwave radiation reaching the surface. The fact that the anomaly also emerges over the eastern part of the Sahel is consistent with the latitudinal coherency of TOTSR at the decadal time scale noted above (Fig. 9a).

An increase of the frequency of light rainfall events (R1mm and R10mm) and heavy rainfall events (R20mm and R75p) in Senegal is also accompanied by a decrease of temperatures in the Sahel and Ethiopia regions (Figs. 8c,e,f,g). The decrease of temperatures is more pronounced for the light (R1mm and R10mm) than for the heavy (R20mm and R75p) rainfall events. Conversely, an increase of the number of dry days (NDD) is associated with a widespread increase of temperatures over land, from Senegal to Ethiopia, over the northern part of the Gulf of Guinea and in central Africa (Fig. 8b) while an increase of the frequency of extreme rainfall events (R95p) and the mean intensity of rainfall events (SDII) is associated with a weak, even insignificant decrease of temperatures in these regions (Figs. 8d,h). In addition, as the number of extreme rainfall events over a season is low, one can expect that R95p might have a weaker effect on land surface temperatures than the other indices, when integrated over the season. Beyond this difference, the pattern of correlations with surface air temperatures is remarkably similar between indices, showing that the same mechanism could be at play.

The correlations with LST fields also show a significant increase of land temperatures over eastern Europe, northern Mexico, the southern United States, East Asia, and over the Mediterranean and surrounding regions (Figs. 8a,c–h). The increase is more significant for the heavy and extreme rainfall events than the light ones. As commented above, these events also have an SST pattern more similar to the AMV, in particular with stronger anomalies on its tropical North Atlantic part (Sutton and Hodson 2005; Ruprich-Robert et al. 2018; Monerie et al. 2021). The warm temperatures over the east of the Mediterranean surrounding regions may be a response to SST warming in the eastern Mediterranean Sea (Fontaine et al. 2010). Note, however, that the changes in Mediterranean SSTs can also be directly impacted by anthropogenic forcings such as aerosols (e.g., Nabat et al. 2014) and greenhouse gases (e.g., Park et al. 2016). This may also modulate land temperatures around the Mediterranean Sea.

c. *Sources and mechanisms of decadal variability of the timing of the Senegalese monsoon season*

In the following, we present results related to the timing of the rainy season: the onset date (SDrs), cessation date (EDrs), and the length of the rainy season (Lrs) in Senegal (Figs. 10 and 11).

Quite distinctly from the rainfall frequency indices, the SST anomalies related to decadal changes in the timing of the rainy season show widespread signals in the tropical Pacific and Indian oceans, while correlations are very weak and mostly statistically insignificant in the tropical Atlantic (Fig. 10). The overall pattern is reminiscent of the IPO (e.g., Mohino et al. 2011a), suggesting that a positive IPO leads to late onset, an early cessation, and an overall shorter rainy season.

Cooler continental surface temperature over Africa, especially over the Sahel and Ethiopia, are related to a longer rainy season (Fig. 10c), consistent with the local mechanism described in section 4b, where a longer rainy season could provide more rainfall locally and thereby explain the cooler anomalies. Although the patterns in Fig. 10 are similar, the particular connection of the length of the rainy season with local surface temperatures seems to come from an earlier onset of the monsoon season (Fig. 10a) rather than a later cessation (Fig. 10b). Figure 10 also shows a decrease in surface temperature over other tropical areas, such as northern South America, Southeast Asia, and western Australia that could be due to the effects of IPO on these regions (e.g., Dong and Dai 2015).

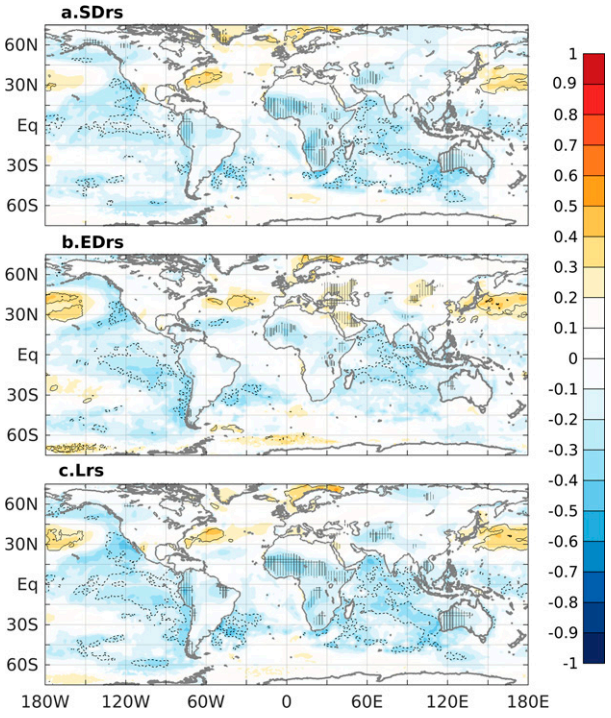

FIG. 10. As in Fig. 8, but for the (a) SDrs, (b) EDrs, and (c) Lrs rainfall indices.

Consistently, the correlations of the decadal variability of indices related to the timing of the monsoon show distinctly different correlation patterns with SLP and mean rainfall anomalies (Fig. 11) than what was found in section 4b. Rainfall anomalies show weak correlations mainly restricted to the Sahel region. This suggests the early onset, late cessation, and increased rainy season are only and moderately related to a local increase of the total seasonal rainfall amount. This could be due to the fact that the definition of the onset and cessation dates of the rainy season used in this study are specifically adapted for West Africa (section 3b). This result is also consistent with the cooler Sahel surface temperature previously noted (Fig. 10). There are no clear correlations over Brazil, suggesting that in this case the decadal variability is not related to an ITCZ meridional shift, which is consistent with the lack of an interhemispheric SST gradient in the Atlantic (Fig. 10). While correlations with SST anomalies were prominent over the tropical Pacific and Indian Oceans (Fig. 10), the SLP signals are mainly restricted to the African and tropical Atlantic sectors (Fig. 11). Such results could again be related to the lack of available SLP data over most of the tropical

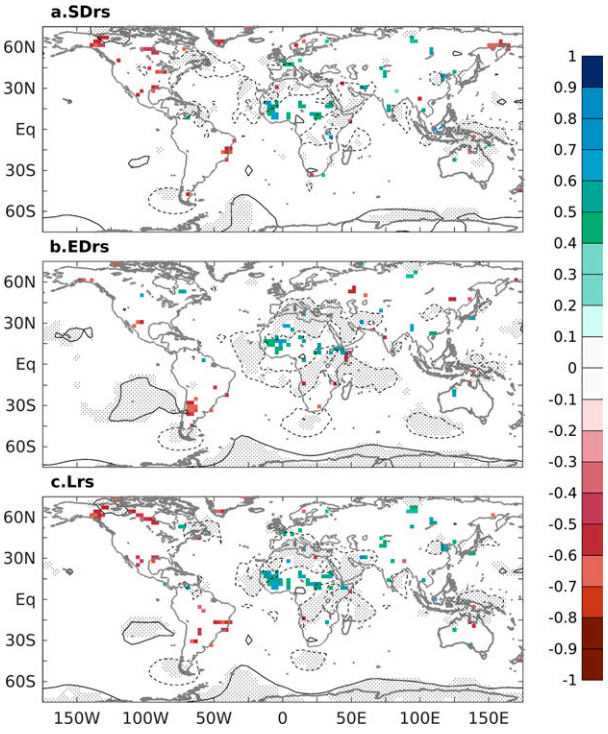

FIG. 11. As in Fig. 9, but for the (a) SDrs, (b) EDrs, and (c) Lrs rainfall indices.

Pacific and Indian Oceans for a great part of the twentieth century (Allan and Ansell 2006). In striking contrast with Fig. 9, Fig. 11 shows a lack of significant signal over the North Atlantic, which is consistent with the overall SST pattern in the region (Fig. 10). Conversely, SLP correlations are statistically significant over the Mediterranean Sea and especially over the Sahara, north of 20°N. The results suggest that the link between the negative phase of the IPO highlighted in Fig. 10 and a longer rainy season, due to both an earlier monsoon onset and a later cessation, could be linked with negative SLP anomalies over the Sahara. In this regard, Lavaysse et al. (2009) showed that the Saharan heat low onset was nearly coincidental with the onset of the WAM. However, whether the negative SLP anomalies in Fig. 11 are related to a stronger Saharan heat low (Biasutti et al. 2009) or a northern shift of it (Shekhar and Boos 2017) cannot be addressed without further analysis of modelled or reanalysis mid-tropospheric data, which is beyond the scope of the present work.

5. Conclusions

We analyzed the decadal variability of a set of rainfall indices over Senegal during the twentieth century and the possible oceanic teleconnection mechanisms associated with it. We focused on the ETCCDI indices related to the frequency and the mean intensity of rainfall events, as well as rainfall indices related to the timing of the rainy season. The analysis of the decadal variability of indices is based on a century-long dataset of daily rainfall collected at different stations over Senegal.

The quantification of available daily data at each station allows us to identify and isolate 24 stations that have more than 80% of available data over the entire 1918–2000 period. The assessment of the homogeneity of the recordings of the 24 pre-selected stations showed that 18 stations were initially homogeneous, an additional four stations were homogeneous after one correction, and two stations remained inhomogeneous after correction. The two latter were omitted for the rest of the study.

The time average of the total summer rainfall over the period 1918–2000 confirms that the highest values of TOTSR are observed in the south of Senegal and the weakest ones to the north, in agreement with Salack et al. (2014). A similar spatial pattern is observed for indices representing the frequency of rainfall events of more than 1 mm and 10 mm (the frequency of light rainfall events), more than 20 mm and above the 75th percentile (the frequency of heavy rainfall events), and above the 95th percentile (the frequency of extreme rainfall events), as well as the mean intensity of rainfall events (SDII). Conversely, the number of dry days is, rather logically, highest in the north and lowest in the south of the country. In addition, a late onset date (SDrs) and an earlier cessation date (EDrs), leading to a shorter rainy season (Lrs) are observed in the north of Senegal compared to the south.

The main mode of variability of the various stations shows that rainfall indices exhibit the same sign load throughout Senegal, even though some of them (e.g., the total seasonal rainfall and the 95th percentile of rainfall of rainy days) present a north-to-south increasing pattern, whereas others (e.g., the onset date of the rainy season) rather show an east–west gradient. The decadal variability of total seasonal rainfall, as well as the frequency and intensity of rainfall events is characterized by a wet period in the 1930s and 1950s followed by a dry period in the 1970s and 1990s, similar to the decadal signal of rainfall in the Sahel during the twentieth century, shown by previous studies (e.g., Giannini et al. 2003; Mohino et al. 2011a). However, for the first time, we show that the rainfall indices related to the timing of the rainy season (SDrs, EDrs, and Lrs) exhibit comparatively fewer decadal modulations than those related to the amplitude and frequency of rainfall events.

The teleconnection mechanism explaining the decadal variability of the rainfall characteristics in Senegal share common features among the different indices analyzed. The warm SSTs over the North Atlantic Ocean and Mediterranean Sea related to a warm phase of the Atlantic multidecadal variability (AMV) are associated with a decrease in pressure over the northern Atlantic, a northward shift of the intertropical convergence zone (ITCZ), and an increase of the seasonal rainfall amount and the frequency and intensity of rainfall events. The decadal changes in the timing of the rainy season (i.e., SDrs, EDrs, and Lrs) however seem to be more related to the interdecadal Pacific oscillation (IPO), in which a positive phase leads to a late onset date, an early cessation date, and an overall shorter rainy season in Senegal. Note however that the somewhat different definitions of the onset and cessation dates of the rainy season based on Marteau's (2010) criteria contain slightly more decadal modulations (from 20% to 25% on average) than those based on the definitions of Sivakumar (1988). In addition, the oceanic teleconnections associated

with the decadal changes are stronger over the North Atlantic and Mediterranean Sea and slightly weaker over the Pacific and Indian Oceans with this alternative definition (not shown). This suggests that the results related to the timing of the monsoon season are sensitive to the definitions of onset and cessation dates of the rainy season (Bombardi et al. 2020) and may require further analysis to test their robustness.

The increase in total seasonal rainfall (TOTSR), frequency of light rainfall events (R1mm and R10mm), and heavy rainfall events (R20mm and R75p) in Senegal is accompanied by a significant decrease of land surface temperature (LST) over the Sahel, while the increase in frequency of the extreme rainfall events (R95p) and mean intensity of rainfall events (SDII) is associated with a modest or even not significant decrease of temperatures over the Sahel.

An in-depth understanding of the associated mechanism was here limited by the lack of observations. Future studies using reanalysis or model simulations are needed. Furthermore, Wang et al. (2021) recently showed that the intensity and frequency of extreme rainfall events have significantly increased in all monsoon regions. If climate simulations prove useful to represent these rainfall characteristics, it would be very interesting for local users to use them to assess the future evolution of the WAM using climate scenarios.

Acknowledgments. Aissatou Badji benefited from support of the Service de Coopération et d'Action Culturelle of the French Embassy in Senegal and the ERASMUS+ program of the European Union. This work was also supported by the Laboratoire Mixte International ECLAIRS2 (IRD) and the UCM XVII call for cooperation and sustainable development. Elsa Mohino also acknowledges the European Commission TRIATLAS (No. 817578) and Spanish Ministry Science and Innovation DISTROPIA (PID2021-125806NB-100) projects. The authors also thank the two anonymous reviewers for their helpful comments and suggestions that have contributed to improve the manuscript.

Data availability statement. CRU TS is available from the Centre for Environmental Data Analysis (CEDA; http://data.ceda.ac.uk//badc/cru/data/cru_ts/), and from the CRU website https://crudata.uea.ac.uk/cru/data/hrg/, as cited by Harris et al. (2020). Sea surface temperature (SST) data are available online at https://www.metoffice.gov.uk/hadobs/hadisst/data/download.html. Land surface temperature (LST) data are available at http://berkeleyearth.org/archive/data/. Sea level pressure (HadSLP2) data can be downloaded from http://hadobs.metoffice.com/hadslp2/.

REFERENCES

Aguilar, E., and Coauthors, 2009: Changes in temperature and precipitation extremes in western central Africa, Guinea Conakry, and Zimbabwe, 1955–2006. *J. Geophys. Res.*, **114**, D02115, https://doi.org/10.1029/2008JD011010.

Alexandersson, H., 1986: A homogeneity test applied to precipitation data. *J. Climatol.*, **6**, 661–675, https://doi.org/10.1002/joc.3370060607.

Allan, R., and T. Ansell, 2006: A new globally complete monthly historical gridded mean sea level pressure dataset (HadSLP2): 1850–2004. *J. Climate*, **19**, 5816–5842, https://doi.org/10.1175/JCLI3937.1.

Biasutti, M., 2013: Forced Sahel rainfall trends in the CMIP5 archive. *J. Geophys. Res. Atmos.*, **118**, 1613–1623, https://doi.org/10.1002/jgrd.50206.

——, 2019: Rainfall trends in the African Sahel: Characteristics, processes, and causes. *Wiley Interdiscip. Rev.: Climate Change*, **10**, e591, https://doi.org/10.1002/wcc.591.

——, A. H. Sobel, and S. J. Camargo, 2009: The role of the Sahara low in summertime Sahel rainfall variability and change in the CMIP3 models. *J. Climate*, **22**, 5755–5771, https://doi.org/10.1175/2009JCLI2969.1.

——, and Coauthors, 2018: Global energetics and local physics as drivers of past, present and future monsoons. *Nat. Geosci.*, **11**, 392–400, https://doi.org/10.1038/s41561-018-0137-1.

Blanchet, J., C. Aly, T. Vischel, G. Panthou, Y. Sané, and M. Diop Kane, 2018: Trend in the co-occurrence of extreme daily rainfall in West Africa since 1950. *J. Geophys. Res. Atmos.*, **123**, 1536–1551, https://doi.org/10.1002/2017JD027219.

Bombardi, R. J., V. Moron, and J. S. Goodnight, 2020: Detection, variability, and predictability of monsoon onset and withdrawal dates: A review. *Int. J. Climatol.*, **40**, 641–667, https://doi.org/10.1002/joc.6264.

Bonfils, C. J. W., B. D. Santer, J. C. Fyfe, K. Marvel, T. J. Phillips, and S. R. H. Zimmerman, 2020: Human influence on joint changes in temperature, rainfall and continental aridity. *Nat. Climate Change*, **10**, 726–731, https://doi.org/10.1038/s41558-020-0821-1.

Diakhate, M., B. Rodriguez-Fonseca, I. Gomera, E. Mohino, A. L. Dieng, and A. T. Gaye, 2019: Oceanic forcing on interannual variability of Sahel heavy and moderate daily rainfall. *J. Hydrometeor.*, **20**, 14, https://doi.org/10.1175/JHM-D-18-0035.1.

Dong, B., and A. Dai, 2015: The influence of the interdecadal Pacific oscillation on temperature and precipitation over the globe. *Climate Dyn.*, **45**, 2667–2681, https://doi.org/10.1007/s00382-015-2500-x.

Dunning, C. M., E. C. L. Black, and R. P. Allan, 2016: The onset and cessation of seasonal rainfall over Africa. *J. Geophys. Res. Atmos.*, **121**, 11 405–11 424, https://doi.org/10.1002/2016JD025428.

Ebisuzaki, W., 1997: A method to estimate the statistical significance of a correlation when the data are serially correlated. *J. Climate*, **10**, 2147–2153, https://doi.org/10.1175/1520-0442(1997)010<2147:AMTETS>2.0.CO;2.

Fall, S., D. Niyogi, and F. H. M. Semazzi, 2006: Analysis of mean climate conditions in Senegal (1971–98). *Earth Interact.*, **10**, 1–40, https://doi.org/10.1175/EI158.1.

Folland, C. K., T. N. Palmer, and D. E. Parker, 1986: Sahel rainfall and worldwide sea temperatures, 1901–85. *Nature*, **320**, 602–607, https://doi.org/10.1038/320602a0.

Fontaine, B., and Coauthors, 2010: Impacts of warm and cold situations in the Mediterranean basins on the West African monsoon: Observed connection patterns (1979–2006) and climate simulations. *Climate Dyn.*, **35**, 95–114, https://doi.org/10.1007/s00382-009-0599-3.

——, P. A. Monerie, M. Gaetani, and P. Roucou, 2011: Climate adjustments over the African-Indian monsoon regions accompanying Mediterranean Sea thermal variability. *J. Geophys. Res.*, **116**, D23122, https://doi.org/10.1029/2011JD016273.

Gaetani, M., B. Fontaine, P. Roucou, and M. Baldi, 2010: Influence of the Mediterranean Sea on the West African monsoon: Intraseasonal variability in numerical simulations. *J. Geophys. Res.*, **115**, D24115, https://doi.org/10.1029/2010JD014436.

Giannini, A., and A. Kaplan, 2019: The role of aerosols and greenhouse gases in Sahel drought and recovery. *Climatic Change*, **152**, 449–466, https://doi.org/10.1007/s10584-018-2341-9.

——, R. Saravanan, and P. Chang, 2003: Oceanic forcing of Sahel rainfall on interannual to interdecadal time scales. *Science*, **302**, 1027–1030, https://doi.org/10.1126/science.1089357.

——, M. Biasutti, I. M. Held, and A. H. Sobel, 2008: A global perspective on African climate. *Climatic Change*, **90**, 359–383, https://doi.org/10.1007/s10584-008-9396-y.

——, S. Salack, T. Lodoun, A. Ali, A. T. Gaye, and O. Ndiaye, 2013: A unifying view of climate change in the Sahel linking intra-seasonal, interannual and longer time scales. *Environ. Res. Lett.*, **8**, 024010, https://doi.org/10.1088/1748-9326/8/2/024010.

González-Rouco, J. F., J. L. Jiménez, V. Quesada, and F. Valero, 2001: Quality control and homogeneity of precipitation data in the southwest of Europe. *J. Climate*, **14**, 964–978, https://doi.org/10.1175/1520-0442(2001)014<0964:QCAHOP>2.0.CO;2

Harris, I., T. J. Osborn, P. Jones, and D. Lister, 2020: Version 4 of the CRU TS monthly high-resolution gridded multivariate climate dataset. *Sci. Data*, **7**, 109, https://doi.org/10.1038/s41597-020-0453-3

Hirasawa, H., P. J. Kushner, M. Sigmond, J. Fyfe, and C. Deser, 2020: Anthropogenic aerosols dominate forced multidecadal Sahel precipitation change through distinct atmospheric and oceanic drivers. *J. Climate*, **33**, 10187–10204, https://doi.org/10.1175/JCLI-D-19-0829.1.

Hountondji, Y.-C., F. De Longueville, and P. Ozer, 2011: Trends in extreme rainfall events in Benin (West Africa), 1960–2000, https://orbi.uliege.be/handle/2268/96112.

Janicot, S., and Coauthors, 2011: Intraseasonal variability of the West African monsoon. *Atmos. Sci. Lett.*, **12**, 58–66, https://doi.org/10.1002/asl.280.

Kitoh, A., E. Mohino, Y. Ding, K. Rajendran, T. Ambrizzi, J. Marengo, and V. Magaña, 2020: Combined oceanic influences on continental climates. *Interacting Climates of Ocean Basins*. C. R. Mechoso, Ed. , Cambridge University Press, 216–257, https://doi.org/10.1017/9781108610995.008.

Knight, J. R., C. K. Folland, and A. A. Scaife, 2006: Climate impacts of the Atlantic multidecadal oscillation. *Geophys. Res. Lett.*, **33**, L17706, https://doi.org/10.1029/2006GL026242.

Lavaysse, C., C. Flamant, S. Janicot, D. J. Parker, J. P. Lafore, B. Sultan, and J. Pelon, 2009: Seasonal evolution of the West African heat low: A climatological perspective. *Climate Dyn.*, **33**, 313–330, https://doi.org/10.1007/s00382-009-0553-4.

Le Barbé, L., and T. Lebel, 1997: Rainfall climatology of the HAPEX-Sahel region during the years 1950–1990. *J. Hydrol.*, **188–189**, 43–73, https://doi.org/10.1016/S0022-1694(96)03154-X

——, ——, and D. Tapsoba, 2002: Rainfall variability in West Africa during the years 1950–90. *J. Climate*, **15**, 187–202, https://doi.org/10.1175/1520-0442(2002)015<0187:RVIWAD>2.0.CO;2.

Lebel, T., and A. Ali, 2009: Recent trends in the central and western Sahel rainfall regime (1990–2007). *J. Hydrol.*, **375**, 52–64, https://doi.org/10.1016/j.jhydrol.2008.11.030

Le Houerou, H., 1992: Relations entre la variabilité des précipitations et celle des productions primaire et secondaire en zone aride. 24 pp., https://www.documentation.ird.fr/hor/fdi:37358.

Liebmann, B., I. Bladé, G. N. Kiladis, L. M. V. Carvalho, G. B. Senay, D. Allured, S. Leroux, and C. Funk, 2012: Seasonality of African precipitation from 1996 to 2009. *J. Climate*, **25**, 4304–4322, https://doi.org/10.1175/JCLI-D-11-00157.1.

Lodoun, T., A. Giannini, P. S. Traoré, L. Somé, M. Sanon, M. Vaksmann, and J. M. Rasolodimby, 2013: Changes in seasonal descriptors of precipitation in Burkina Faso associated with late 20th century drought and recovery in West Africa. *Environ. Dev.*, **5**, 96–108, https://doi.org/10.1016/j.envdev.2012.11.010.

Longueville, F. D., Y. C. Hountondji, I. Kindo, F. Gemenne, and P. Ozer, 2016: Long-term analysis of rainfall and temperature data in Burkina Faso (1950–2013). *Int. J. Climatol.*, **36**, 13, https://doi.org/10.1002/joc.4640.

Losada, T., B. Rodríguez-Fonseca, S. Janicot, S. Gervois, F. Chauvin, and P. Ruti, 2010: A multi-model approach to the Atlantic equatorial mode: Impact on the West African monsoon. *Climate Dyn.*, **35**, 29–43, https://doi.org/10.1007/s00382-009-0625-5.

Lu, J., and T. L. Delworth, 2005: Oceanic forcing of the late 20th century Sahel drought. *Geophys. Res. Lett.*, **32**, L22706, https://doi.org/10.1029/2005GL023316.

Ly, M., S. B. Traore, A. Alhassane, and B. Sarr, 2013: Evolution of some observed climate extremes in the West African Sahel. *Wea. Climate Extremes*, **1**, 19–25, https://doi.org/10.1016/j.wace.2013.07.005.

Maloney, E. D., and J. Shaman, 2008: Intraseasonal variability of the West African monsoon and Atlantic ITCZ. *J. Climate*, **21**, 2898–2918, https://doi.org/10.1175/2007JCLI1999.1.

Marteau, R., 2010: Cohérence Spatiale et previsibilité potentielle des descripteurs intrasaisonniers de la saison des pluies en Afrique Soudano-Sahélienne: Application à la culture du mil dans la région de Niamey. Ph.D. thesis, Université de Bourgogne, 242 pp.

——, V. Moron, and N. Philippon, 2009: Spatial coherence of monsoon onset over western and central Sahel (1950–2000). *J. Climate*, **22**, 1313–1324, https://doi.org/10.1175/2008JCLI2383.1.

Martin, E. R., and C. D. Thorncroft, 2013: The impact of the AMO on the West African monsoon annual cycle. *Quart. J. Roy. Meteor. Soc.*, **140**, 31–46, https://doi.org/10.1002/qj.2107.

Marvel, K., M. Biasutti, and C. Bonfils, 2020: Fingerprints of external forcings on Sahel rainfall: Aerosols, greenhouse gases, and model–observation discrepancies. *Environ. Res. Lett.*, **15**, 084023, https://doi.org/10.1088/1748-9326/ab858e.

Misra, A. N., and M. Misra, 1991: Physiological responses of pearl millet to agroclimatic conditions. *Environmental Contamination and Hygiene*. Jagmandir Books, 165–175.

Mohino, E., S. Janicot, and J. Bader, 2011a: Sahel rainfall and decadal to multi-decadal sea surface temperature variability. *Climate Dyn.*, **37**, 419–440, https://doi.org/10.1007/s00382-010-0867-2.

——, B. Rodríguez-Fonseca, T. Losada, S. Gervois, S. Janicot, J. Bader, P. Ruti, and F. Chauvin, 2011b: Changes in the interannual SST-forced signals on West African rainfall. AGCM intercomparison. *Climate Dyn.*, **37**, 1707–1725, https://doi.org/10.1007/s00382-011-1093-2.

Monerie, P.-A., J. Robson, B. Dong, D. Hodson, and N. P. Klingaman, 2019: Effect of the Atlantic multidecadal variability on the global monsoon. *Geophys. Res. Lett.*, **46**, 1765–1775, https://doi.org/10.1029/2018GL080903.

——, ——, ——, and ——, 2021: Role of the Atlantic multidecadal variability in modulating East Asian climate. *Climate Dyn.*, **56**, 381–398, https://doi.org/10.1007/s00382-020-05477-y.

Moron, V., A. W. Robertson, and M. N. Ward, 2006: Seasonal predictability and spatial coherence of rainfall characteristics in the tropical setting of Senegal. *Mon. Wea. Rev.*, **134**, 3248–3262, https://doi.org/10.1175/MWR3252.1.

Nabat, P., S. Somot, M. Mallet, A. Sanchez-Lorenzo, and M. Wild, 2014: Contribution of anthropogenic sulfate aerosols to the changing Euro-Mediterranean climate since 1980. *Geophys. Res. Lett.*, **41**, 5605–5611, https://doi.org/10.1002/2014GL060798.

New, M., and Coauthors, 2006: Evidence of trends in daily climate extremes over southern and West Africa. *J. Geophys. Res.*, **111**, D14102, https://doi.org/10.1029/2005JD006289.

Nieto, R., L. Gimeno, and R. M. Trigo, 2006: A Lagrangian identification of major sources of Sahel moisture. *Geophys. Res. Lett.*, **33**, L18707, https://doi.org/10.1029/2006GL027232.

North, G. R., T. L. Bell, R. F. Cahalan, and F. J. Moeng, 1982: Sampling errors in the estimation of empirical orthogonal functions. *Mon. Wea. Rev.*, **110**, 699–706, https://doi.org/10.1175/1520-0493(1982)110<0699:SEITEO>2.0.CO;2.

Oladipo, E. O., and J. D. Kyari, 1993: Fluctuations in the onset, termination and length of the growing season in northern Nigeria. *Theor. Appl. Climatol.*, **47**, 241–250, https://doi.org/10.1007/BF00866245.

Ozer, A., and P. Ozer, 2005: Désertification au Sahel: Crise climatique ou anthropique? *Bull. Seances Acad. Roy. Sci. Outre Mer.*, **51**, 395–423, https://orbi.uliege.be/handle/2268/16053.

Ozer, P., Y. C. Hountondji, and O. Laminou Manzo, 2009: Evolution des caractéristiques pluviométriques dans l'est du Niger de 1940 à 2007. *Geo. Eco. Trop.*, **33**, 11–30, https://hdl.handle.net/2268/78267.

Palmer, T. N., 1986: Influence of the Atlantic, Pacific and Indian Oceans on Sahel rainfall. *Nature*, **322**, 251–253, https://doi.org/10.1038/322251a0.

Panthou, G. T., T. Vischel, T. Lebel, G. Quantin, F. Pugin, J. Blanchet, and A. Ali, 2013: From pointwise testing to a regional vision: An integrated statistical approach to detect nonstationarity in extreme daily rainfall. Application to the Sahelian region. *J. Geophys. Res. Atmos.*, **118**, 8222–8237, https://doi.org/10.1002/jgrd.50340.

——, ——, and ——, 2014: Recent trends in the regime of extreme rainfall in the central Sahel. *Int. J. Climatol.*, **34**, 9, https://doi.org/10.1002/joc.3984.

——, and Coauthors, 2018: Rainfall intensification in tropical semi-arid regions: The Sahelian case. *Environ. Res. Lett.*, **13**, 10, https://doi.org/10.1088/1748-9326/aac334.

Park, J., J. Bader, and D. Matei, 2016: Anthropogenic Mediterranean warming essential driver for present and future Sahel rainfall. *Nat. Climate Change*, **6**, 941–945, https://doi.org/10.1038/nclimate3065.

Peyrillé, P., J. P. Lafore, and J. L. Redelsperger, 2007: An idealized two-dimensional framework to study the West African monsoon. Part I: Validation and key controlling factors. *J. Atmos. Sci.*, **64**, 2765–2782, https://doi.org/10.1175/JAS3919.1.

Raicich, F., N. Pinardi, and A. Navarra, 2003: Teleconnections between Indian monsoon and Sahel rainfall and the Mediterranean. *Int. J. Climatol.*, **23**, 173–186, https://doi.org/10.1002/joc.862.

Rayner, N. A. A., D. E. Parker, E. B. Horton, C. K. Folland, L. V. Alexander, D. P. Rowell, E. C. Kent, and A. Kaplan, 2003: Global analyses of sea surface temperature, sea ice, and night marine air temperature since the late nineteenth century. *J. Geophys. Res.*, **108**, 4407, https://doi.org/10.1029/2002JD002670.

Ribeiro, S., J. Caineta, and A. C. Costa, 2016: Review and discussion of homogenisation methods for climate data. *Phys. Chem. Earth*, **94**, 167–179, https://doi.org/10.1016/j.pce.2015.08.007.

Rodríguez-Fonseca, B., and Coauthors, 2011: Interannual and decadal SST-forced responses of the West African monsoon. *Atmos. Sci. Lett.*, **12**, 67–74, https://doi.org/10.1002/asl.308.

——, and Coauthors, 2015: Variability and predictability of West African droughts: A review on the role of sea surface temperature anomalies. *J. Climate*, **28**, 4034–4060, https://doi.org/10.1175/JCLI-D-14-00130.1.

Rohde, R. A., A. Muller, R. Jacobsen, E. Muller, and C. Wickham, 2013: A new estimate of the average Earth surface land temperature spanning 1753 to 2011. *Geoinf. Geostat.: An Overview*, **1**, 1, https://doi.org/10.4172/2327-4581.1000101.

Rowell, D. P., 2001: Teleconnections between the tropical Pacific and the Sahel. *Quart. J. Roy. Meteor. Soc.*, **127**, 1683–1706, https://doi.org/10.1002/qj.49712757512.

——, 2003: The impact of Mediterranean SSTs on the Sahelian rainfall season. *J. Climate*, **16**, 849–862, https://doi.org/10.1175/1520-0442(2003)016<0849:TIOMSO>2.0.CO;2.

——, C. K. Folland, K. Maskell, J. A. Owen, and M. N. Ward, 1992: Modelling the influence of global sea surface temperatures on the variability and predictability of seasonal Sahel rainfall. *Geophys. Res. Lett.*, **19**, 905–908, https://doi.org/10.1029/92GL00939.

——, ——, ——, and M. N. Ward, 1995: Variability of summer rainfall over tropical North Africa (1906–92): Observations and modelling. *Quart. J. Roy. Meteor. Soc.*, **121**, 669–704, https://doi.org/10.1002/qj.49712152311.

Ruprich-Robert, Y., R. Msadek, F. Castruccio, S. Yeager, T. Delworth, and G. Danabasoglu, 2017: Assessing the climate impacts of the observed Atlantic multidecadal variability using the GFDL CM2.1 and NCAR CESM1 global coupled models. *J. Climate*, **30**, 2785–2810, https://doi.org/10.1175/JCLI-D-16-0127.1.

——, T. Delworth, R. Msadek, F. Castruccio, S. Yeager, and G. Danabasoglu, 2018: Impacts of the Atlantic multidecadal variability on North American summer climate and heat waves. *J. Climate*, **31**, 3679–3700, https://doi.org/10.1175/JCLI-D-17-0270.1.

Salack, S., B. Muller, and A. T. Gaye, 2011: Rain-based factors of high agricultural impacts over Senegal. Part I: Integration of local to sub-regional trends and variability. *Theor. Appl. Climatol.*, **106**, 1–22, https://doi.org/10.1007/s00704-011-0414-z.

——, A. Giannini, M. Diakhate, A. T. Gaye, and B. Muller, 2014: Oceanic influence on the sub-seasonal to interannual timing and frequency of extreme dry spells over the West African Sahel. *Climate Dyn.*, **42**, 189–201, https://doi.org/10.1007/s00382-013-1673-4.

Sanogo, S., A. H. Fink, J. A. Omotosho, A. Ba, R. Redl, and V. Ermert, 2015: Spatio-temporal characteristics of the recent rainfall recovery in West Africa. *Int. J. Climatol.*, **35**, 4589–4605, https://doi.org/10.1002/joc.4309.

Sarr, B., 2011: Return of heavy downpours and floods in a context of changing climate. *AGRHYMET Mon. Bull.*, 9–11.

Sarr, M. A., P. Gachon, O. Seidou, C. R. Bryant, J. A. Ndione, and J. Comby, 2015: Inconsistent linear trends in Senegalese rainfall indices from 1950 to 2007. *Hydrol. Sci. J.*, **60**, 1538–1549, https://doi.org/10.1080/02626667.2014.926364.

Schneider, T., T. Bischoff, and G. H. Haug, 2014: Migrations and dynamics of the intertropical convergence zone. *Nature*, **513**, 45–53, https://doi.org/10.1038/nature13636.

Shekhar, R., and W. R. Boos, 2017: Weakening and shifting of the Saharan shallow meridional circulation during wet years of the West African monsoon. *J. Climate*, **30**, 7399–7422, https://doi.org/10.1175/JCLI-D-16-0696.1.

Sillmann, J., V. V. Kharin, X. Zhang, F. W. Zwiers, and D. Bronaugh, 2013: Climate extremes indices in the CMIP5 multimodel ensemble: Part 1. Model evaluation in the present climate. *J. Geophys. Res. Atmos.*, **118**, 1716–1733, https://doi.org/10.1002/jgrd.50203.

Sivakumar, M. V. K., 1988: Predicting rainy season potential from the onset of rains in southern Sahelian and Sudanian climatic zones of West Africa. *Agric. For. Meteor.*, **42**, 295–305, https://doi.org/10.1016/0168-1923(88)90039-1.

——, 1992: Empirical analysis of dry spells for agricultural applications in West Africa. *J. Climate*, **5**, 532–539, https://doi.org/10.1175/1520-0442(1992)005<0532:EAODSF>2.0.CO;2.

Sultan, B., S. Janicot, and A. Diedhiou, 2003: The West African monsoon dynamics. Part I: Documentation of intraseasonal variability. *J. Climate*, **16**, 3389–3406, https://doi.org/10.1175/1520-0442(2003)016<3389:TWAMDP>2.0.CO;2.

——, C. Baron, M. Dingkuhn, B. Sarr, and S. Janicot, 2005: Agricultural impacts of large-scale variability of the West African monsoon. *Agric. For. Meteor.*, **128**, 93–110, https://doi.org/10.1016/j.agrformet.2004.08.005.

Sutton, R. T., and D. L. Hodson, 2005: Atlantic Ocean forcing of North American and European summer climate. *Science*, **309**, 115–118, https://doi.org/10.1126/science.1109496.

Taylor, C. M., and Coauthors, 2017: Frequency of extreme Sahelian storms tripled since 1982 in satellite observations. *Nature*, **544**, 475–478, https://doi.org/10.1038/nature22069.

Taylor, M. H., M. Losch, M. Wenzel, and J. Schröter, 2013: On the sensitivity of field reconstruction and prediction using empirical orthogonal functions derived from gappy data. *J. Climate*, **26**, 9194–9205, https://doi.org/10.1175/JCLI-D-13-00089.1.

Ting, M., Y. Kushnir, R. Seager, and C. Li, 2009: Forced and internal twentieth-century SST trends in the North Atlantic. *J. Climate*, **22**, 1469–1481, https://doi.org/10.1175/2008JCLI2561.1.

Wade, M., J. Mignot, A. Lazar, A. T. Gaye, and M. Carré, 2015: On the spatial coherence of rainfall over the Saloum delta (Senegal) from seasonal to decadal time scales. *Front. Earth Sci.*, **3**, 30, https://doi.org/10.3389/feart.2015.00030.

Wang, B., and Coauthors, 2021: Monsoons climate change assessment. *Bull. Amer. Meteor. Soc.*, **102**, E1–E19, https://doi.org/10.1175/BAMS-D-19-0335.1.

Ward, M. N., 1998: Diagnosis and short-lead time prediction of summer rainfall in tropical North Africa at interannual and multidecadal timescales. *J. Climate*, **11**, 3167–3191, https://doi.org/10.1175/1520-0442(1998)011<3167:DASLTP>2.0.CO;2.

Zhang, R., and T. L. Delworth, 2006: Impact of Atlantic multidecadal oscillations on India/Sahel rainfall and Atlantic hurricanes. *Geophys. Res. Lett.*, **33**, L17712, https://doi.org/10.1029/2006GL026267.